

1966

# Integral Solution for Turbulent Mixing of Two Parallel Air Streams in a Duct

Thomas Fredric Kascoutas

Follow this and additional works at: <https://openprairie.sdstate.edu/etd>

---

## Recommended Citation

Kascoutas, Thomas Fredric, "Integral Solution for Turbulent Mixing of Two Parallel Air Streams in a Duct" (1966). *Electronic Theses and Dissertations*. 3208.  
<https://openprairie.sdstate.edu/etd/3208>

This Thesis - Open Access is brought to you for free and open access by Open PRAIRIE: Open Public Research Access Institutional Repository and Information Exchange. It has been accepted for inclusion in Electronic Theses and Dissertations by an authorized administrator of Open PRAIRIE: Open Public Research Access Institutional Repository and Information Exchange. For more information, please contact [michael.biondo@sdstate.edu](mailto:michael.biondo@sdstate.edu).

INTEGRAL SOLUTION FOR TURBULENT MIXING OF TWO  
PARALLEL AIR STREAMS IN A DUCT

BY

THOMAS FREDRIC KASCOULTAS

A thesis submitted  
in partial fulfillment of the requirements for the  
degree Master of Science, Major in  
Mechanical Engineering, South  
Dakota State University

1966

SOUTH DAKOTA STATE UNIVERSITY LIBRARY

INTEGRAL SOLUTION FOR TURBULENT MIXING OF TWO  
PARALLEL AIR STREAMS IN A DUCT

This thesis is approved as a creditable and independent investigation by a candidate for the degree Master of Science, and is acceptable as meeting the thesis requirements for this degree, but without implying that the conclusions reached by the candidate are necessarily the conclusions of the major department.

## ACKNOWLEDGMENTS

It seems fitting that the author should formally recognize the incalculable assistance of Mr. O. T. Sessions, graduate assistant, who aided in the collection and computation of the data. Further, the counseling of Prof. B. E. Eno aided greatly in the analytical considerations.

TFK



## TABLE OF CONTENTS

Chapter	Page
I. INTRODUCTION.....	1
II. OBJECTIVES.....	5
III. RESEARCH FACILITIES.....	7
IV. DISCUSSION OF NAVIER-STOKES EQUATIONS OF MOTION.....	10
V. REVIEW OF RELATED LITERATURE.....	14
A. Laminar Stability.....	14
B. Phenomenological Theories.....	15
C. Statistical Theories.....	30
VI. ANALYTICAL CONSIDERATIONS.....	33
VII. RESULTS AND DISCUSSION.....	41
A. Developmental Assumptions.....	44
B. Procedural Assumptions.....	45
VIII. CONCLUSIONS AND RECOMMENDATIONS.....	49
BIBLIOGRAPHY.....	51
APPENDIX A.....	53
APPENDIX B.....	66

## LIST OF FIGURES

Figure	Page
1. Idealized Mixing of Parallel Streams.....	3
2. Mixing of Parallel Streams with Upstream Boundary Layers.....	3
3. Schematic of Duct.....	8
4. Prandtl's Mixing Concept.....	17
5. Typical Apparent Shear, Normal and Transverse Turbulence Component Profiles.....	29
6. Comparison of Normal and Transverse Turbulence Components for $u_A = 113$ ft/sec and $u_B = 51$ ft/sec.....	54
7. Normal Turbulence Component Profile for $u_A = u_B = 110$ ft/sec.....	55
8. Apparent Shear Profile for $u_A = u_B = 110$ ft/sec.....	56
9. Normal Turbulence Component Profile for $u_A = u_B = 61.5$ ft/sec.....	57
10. Apparent Shear Profile for $u_A = u_B = 61.5$ ft/sec.....	58
11. Normal Turbulence Component Profile for $u_A = u_B = 39.7$ ft/sec.....	59
12. Apparent Shear Profile for $u_A = u_B = 39.7$ ft/sec.....	60
13. Normal Turbulence Component Profile for $u_A = 113$ ft/sec and $u_B = 51$ ft/sec.....	61
14. Apparent Shear Profile for $u_A = 113$ ft/sec and $u_B = 51$ ft/sec.....	62
15. Normal Turbulence Component Profile for $u_A = 67$ ft/sec and $u_B = 43$ ft/sec.....	63
16. Apparent Shear Profile for $u_A = 67$ ft/sec and $u_B = 43$ ft/sec.....	64
17. Comparison Between Measured and Gortler Velocity Profiles.....	65

Figure

Page

18. X-Wire Probe in a Typical Flow Situation.....	63
---	----

## NOMENCLATURE

- $a(x)$  - distance between jet axis and free stream in top channel  
 $b(x)$  - distance between jet axis and free stream in bottom channel  
 $B$  - width of mixing zone  
 $c$  - ratio between  $a(x)$  and  $b(x)$   
 $c_1$  and  $c_2$  - instantaneous cooling velocity on wires 1 and 2 respectively  
 $C_1$  and  $C_2$  - mean time cooling velocity on wires 1 and 2 respectively  
 $K$  - sensitivity constant  
 $K_G$  - galvanometer constant  
 $K_V$  - voltmeter constant  
 $L$  - Prandtl's mixing length  
 $m$  - velocity ratio between channels  
 $M_1, M_2, M_{1-2}, M_{1+2}$  - random signal voltmeter readings of wire 1,  
     wire 2, wire 1 minus wire 2 and wire 1 plus wire 2, respectively  
 $n$  - wire cooling constant  
 $t$  - time  
 $u$  - velocity in x-direction  
 $u_0$  or  $U$  - free stream velocity  
 $u_m$  and  $u$  - free stream velocity defined by Prandtl  
 $v$  - velocity in y-direction  
 $w$  - velocity in z-direction  
 $x$  - downstream dimension  
 $y$  - transverse dimension  
 $z$  - depth dimension

- $\alpha$  - dimensionless minimum velocity
- $\beta$  - half-angle between wires of X-array
- $\epsilon$  - coefficient of eddy viscosity
- $\rho$  - density
- $\mu$  - laminar viscosity
- $\nu$  - kinematic viscosity
- $\psi$  - stream function
- $\eta$  - dimensionless distance  $y/a$
- $\chi$  - coefficient of turbulent viscosity
- $\tau$  - shearing stress

## CHAPTER I

### INTRODUCTION

Turbulence is characterized by random fluctuating motions in the longitudinal and transverse direction which have macroscopic effects upon the flow pattern. In the study of fluid flow, it is beneficial to visualize motions of particles of different sizes. The particles can be categorized into those of a molecular magnitude and those of a larger scale. The larger scale particles can best be thought of as fluid lumps.

Fundamentally, there are two types of fluid flow (laminar and turbulent). In laminar flow, the fluctuating particles are of a microscopic scale. These particles possess only small amounts of mass and energy, thus their motions will have only microscopic effects upon the flow patterns. In turbulent flow, the fluctuating particles are the fluid lumps. The lumps possess a substantial amount of mass and energy, thus the motion of the lumps will have macroscopic effects upon the flow pattern.

Turbulence can occur in a multiplicity of flow types. Those flow types include: (1) shear flow (which can be subdivided into boundary layer and pipe flow), (2) homogeneous isotropic flow (i.e., downstream of a screen) and (3) jets and mixing regions. In this particular case, a mixing region formed by the merging of two air streams flowing parallel in a duct was studied. This type of study is particularly beneficial in obtaining information concerning turbulence because the laminar effects are negligible with respect to

the turbulent effects. This is true because there is no solid boundary over which the fluid particles will not slip; thus, the velocity gradients are relatively small.

Most analyses of turbulent mixing regions are based upon the assumption that the mixing region will approximate a free, isotropic zone. The terms isotropic and free mean that the turbulent components are not preferential respecting direction nor are the fluctuations bounded by any solid surfaces. A schematic of such an idealized mixing region is shown in Figure 1.<sup>1</sup> Note that the effect of an initial boundary layer is not considered in this idealized case.

It should be emphasized that not all mixing regions formed by merging parallel streams are of a necessity turbulent. The idealized example will usually be laminar initially. It may well be "tripped" into turbulent flow downstream. The precise lower limit of laminar stability has not yet been determined because of lack of understanding concerning the turbulent mechanism. In Figure 1 and for this study, it is assumed that the onset of turbulence occurs relatively quickly, thus eliminating laminar considerations.

Finally, it is felt that a brief portion of this introduction should be devoted to the mathematically expressed relationships which will form the basis for the theory presented here. These relationships are the Navier-Stokes<sup>2-1</sup> equations of motion. The general manner

---

<sup>1</sup>Figures 1-5 will be contained in the text, all subsequent figures will be included in Appendices A and B.

<sup>2</sup>Cited literature will be referenced to the bibliography.

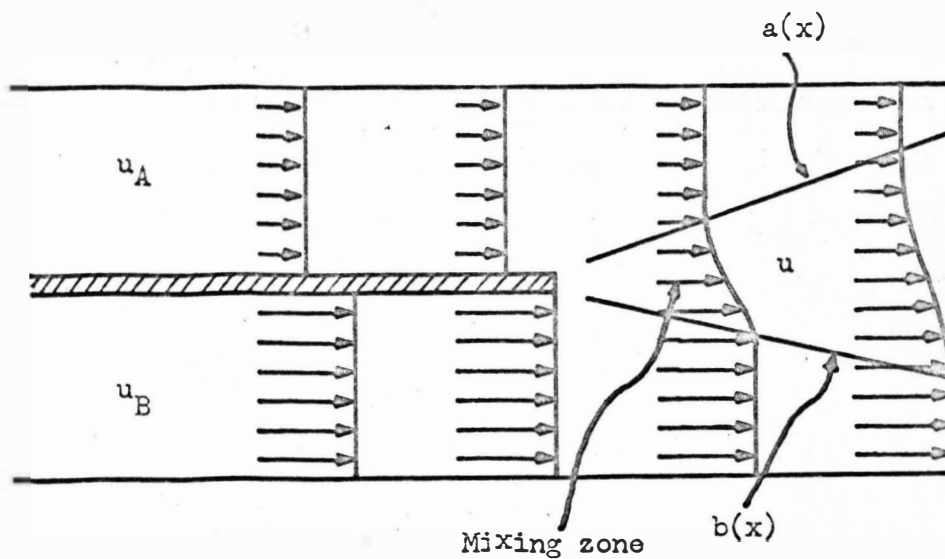


Figure 1. Idealized Mixing of Parallel Streams

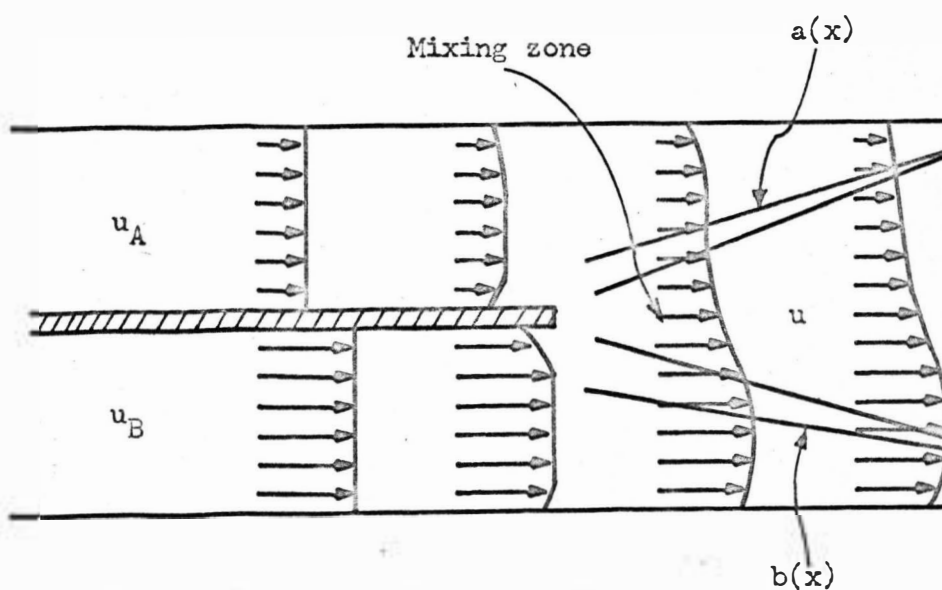


Figure 2. Mixing of Parallel Streams with Upstream Boundary Layers



in which these equations were developed (substitution of Stokes viscosity law<sup>1</sup> into Newton's second law of motion<sup>1</sup>) allows the resolution of nearly any type of motion resulting from a shearing strain. This assumes that sufficient restrictions and boundary conditions can be applied to the general form of the equations.

## CHAPTER II

## OBJECTIVE

The objective of this study is actually two-fold. The first of the proposed goals is the reduction of the Navier-Stokes equations of motion to a form capable of integration. This is to be accomplished through a logical and systematic elimination of those terms not pertinent to the case studied. The accomplishment of this goal is predicated upon the assumption that there exists or can be developed a method of attack which is appropriate to the case. In actual fact, no such method exists or is developed here, precisely because of lack of information concerning the turbulent mixing mechanism. Thus, it was necessary to follow the assumption utilized in the idealized case; namely, that the mixing action is similar to boundary layer action and, therefore, the analysis is similar.

The particular case to be studied is depicted in Figure 2. Note that this example is different than the idealized in that the upstream boundary layer is now a matter of consideration. Thus, the extension of idealized theories to this case is a subject worthy of investigation and contingent upon proof. This analysis and verification will constitute the first object of this thesis.

Once the equation has been reduced and those reducing assumptions checked, the next logical goal is the solution of the equation. Various techniques are available and a section will be devoted to a discussion of those techniques. After determining a method of solution and proceeding with it, it becomes apparent that additional restric-

tions must be placed upon the equations. Assuming the validity of the restrictions, a solution to the equations can be provided. Once again experimental verification will be required both to check the procedural assumptions and the final solution.

## CHAPTER III

### RESEARCH EQUIPMENT

The facilities utilized to obtain experimental information for this study are essentially those described by Iverson<sup>2</sup> and Goel<sup>3</sup>. The duct itself is 10" x 10" cross section. It is schematically depicted in Figure 3. The new slots which were cut in the duct were necessary before the probes could be inserted at the proper orientation to measure the desired components.

Goel mounted screens (see Figure 3) at a point 1-1/4" upstream of the end of the splitter plate. Preliminary measurements indicated that the level of turbulence in the region downstream of the plate was such that the effects of the screen would overshadow those of the mixing zone. It was felt that the excessive turbulence was attributable to the proximity of the screens to the mixing region. Thus the screens were moved to about 15" upstream of the trailing edge of the splitter plate. It was hoped that the turbulent boundary layer would approximate the characteristics of a natural boundary layer in this added distance.

The heart of the measuring apparatus is the hot-wire anemometer. After attaching the appropriate sensing device, the anemometer is capable of indicating an average velocity and reproducing velocity fluctuations as voltage pulses. These voltage pulses are read on a random signal voltmeter. This unit averages the pulses over a 16 second interval.

The measuring capacity of the facility has been considerably

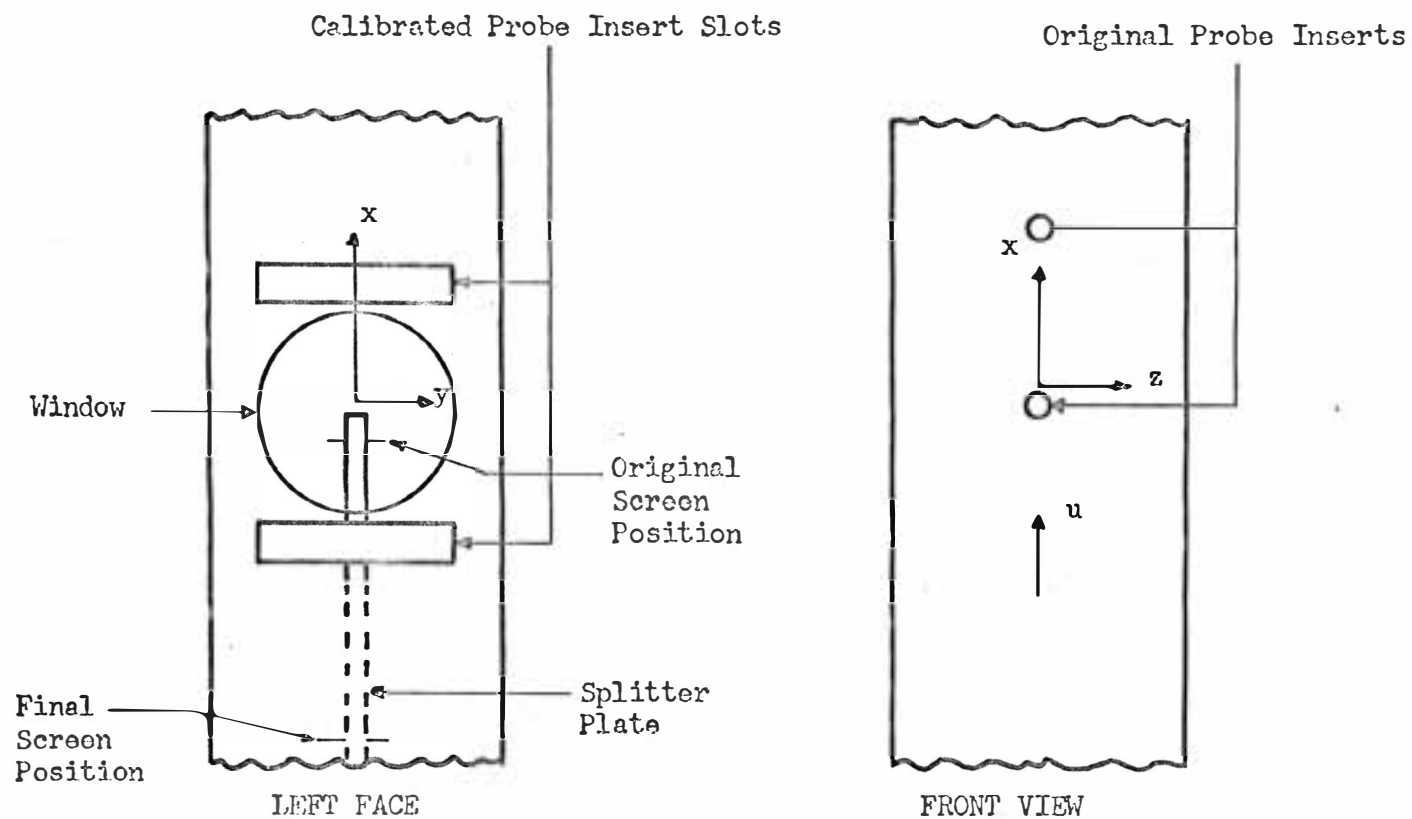


Figure 3. Schematic of Duct

expanded through the addition of the Flow Corporation Sum and Difference Control Unit. This unit contains its own current supply; thus, two sensing devices can simultaneously produce voltage pulses which can be fed to the random signal voltmeter. These sensing devices (thin wires) can be mounted on separate probes measuring normal components for the purpose of obtaining either longitudinal or transverse correlation coefficients. They may also be mounted, as was done in the present study, on the same probe approximately perpendicular to one another. This X-array, as it is called, allows measurement of the apparent shear stress component. The apparent shear component is the mean time average of the product of the normal and transverse fluctuations at a point.

## CHAPTER IV

## DISCUSSION OF THE EQUATIONS OF MOTION

The Navier-Stokes equations of motion<sup>1</sup> mentioned in the introduction will be discussed more fully in this section. This will lay the foundation for the analysis of the following sections.

The equations of motion combined with the continuity equation<sup>1</sup> form the most powerful tools available to the fluid dynamicist. The following are these equations in vector form.

$$\frac{d\rho}{dt} + \text{div}(\rho \bar{V}) = 0 \quad (4-1)$$

$$\rho \frac{D\bar{V}}{Dt} = \frac{1}{3} \mu \bar{V} (\text{div} \bar{V}) + \mu \nabla^2 \bar{V} - \nabla P \quad (4-2)$$

Equation (4-1) is the continuity equation and (4-2) is the equation of motion. Obviously, these equations will not be readily solved in this form. Thus, it is necessary to make some restrictive assumptions.

Air flowing at speeds less than Mach 0.3 is considered incompressible. Since the flows encountered in the present study are well within that bound, it is possible to write

$$\text{div} \bar{V} = 0 \quad (4-3)$$

This eliminates the first term on the right hand side of (4-2) from consideration in this study.

The equations of motion are valid for turbulent flow if instantaneous values are used. Represent any of the fluctuating quantities in (4-2) as B, this leads to

$$B = \bar{B} + B' \quad (4-4)$$

or the instantaneous value of  $B$  is equal to the mean time average plus the fluctuating component of  $B$ . The mean time average is defined as

$$\bar{B} = \frac{1}{\Delta t} \int_t^{t+\Delta t} B \, dt \quad (4-5)$$

where  $\Delta t$ , according to Hunt<sup>4</sup>, is defined as a time interval which is large compared to the time scale of the largest eddies present.

Thus it follows that

$$\frac{1}{\Delta t} \int_t^{t+\Delta t} B' \, dt = \bar{B'} = 0 \quad (4-6)$$

Now rewrite (4-2) in cartesian coordinates. Substitute instantaneous values into (4-2) as indicated in (4-4). Take the mean time average of the equations and substitute from continuity in a manner similar to Shames. Finally transpose the fluctuating components to the right hand side of the equation and write

$$\frac{\partial \bar{u}}{\partial t} + \bar{u} \frac{\partial \bar{u}}{\partial x} + \bar{v} \frac{\partial \bar{u}}{\partial y} + \bar{w} \frac{\partial \bar{u}}{\partial z} = -\frac{1}{\rho} \frac{\partial \bar{p}}{\partial x} + \nu \nabla^2 \bar{u} - \left[ \frac{\partial (\overline{u^2})}{\partial x} + \frac{\partial (\overline{uv})}{\partial y} + \frac{\partial (\overline{uw})}{\partial z} \right] \quad (4-7)$$

$$\frac{\partial \bar{v}}{\partial t} + \bar{u} \frac{\partial \bar{v}}{\partial x} + \bar{v} \frac{\partial \bar{v}}{\partial y} + \bar{w} \frac{\partial \bar{v}}{\partial z} = -\frac{1}{\rho} \frac{\partial \bar{p}}{\partial y} + \nu \nabla^2 \bar{v} - \left[ \frac{\partial (\overline{uv})}{\partial x} + \frac{\partial (\overline{v^2})}{\partial y} + \frac{\partial (\overline{vw})}{\partial z} \right] \quad (4-8)$$

$$\frac{\partial \bar{w}}{\partial t} + \bar{u} \frac{\partial \bar{w}}{\partial x} + \bar{v} \frac{\partial \bar{w}}{\partial y} + \bar{w} \frac{\partial \bar{w}}{\partial z} = -\frac{1}{\rho} \frac{\partial \bar{p}}{\partial z} + \nu \nabla^2 \bar{w} - \left[ \frac{\partial (\overline{uw})}{\partial x} + \frac{\partial (\overline{vw})}{\partial y} + \frac{\partial (\overline{w^2})}{\partial z} \right] \quad (4-9)$$

The final general assumptions which are applicable to turbulent mixing zones will be considered at this time. The first restriction to be applied is almost mandatory from the standpoint of reducing the



motion equations (4-7), (4-8) and (4-9) to a form capable of integration. This is the assumption of two-dimensionality. It is true in the idealized case of Figure 1 but is made with certain reservations for the present study. Discussion of possible effects of this limitation will be reserved for the results and discussion. The effect of this assumption is to eliminate (4-9) and all  $\bar{w}$  and  $\frac{\partial}{\partial z}$  terms in (4-7) and (4-8).

The second assumption is that  $\frac{\partial \bar{p}}{\partial x}$  and  $\frac{\partial \bar{p}}{\partial y}$  can be neglected. Experiment<sup>5</sup> has shown that  $\frac{\partial \bar{p}}{\partial y} < \frac{\partial \bar{p}}{\partial x}$  and that  $\frac{\partial \bar{p}}{\partial x}$  is negligible for short distances downstream. Since the distance over which measurements will be taken in this study is relatively short (10"), and since pressure probe readings at various points appeared nearly constant, the assumption seems reasonable. The effect of this assumption is to eliminate the first terms on the right hand side of (4-7) and (4-8).

At this point, apply the restriction of steady state flow to the equations (4-7) and (4-8). There is no reason to suspect that  $\bar{u}$  or  $\bar{v}$  will vary with time. This removes the first terms of the left hand side of (4-7) and (4-8) from consideration.

Experiment<sup>6</sup> has shown that the velocity gradients with respect to  $y$  in a mixing zone are much less severe than those gradients characteristic of flow over solid boundaries. This lessening of the severity of the gradient is due to the fact that the fluid layers will stick to one another. This adhesion of the fluid layers will cause the velocity profile to flatten out at some large distance downstream of the trailing edge of the splitter plate. The combination of this

dampening of the velocity gradient and the inherently small viscosity of air produces the second assumption. That assumption is that the second terms on the right hand side of equations (4-7) and (4-8) can be dropped from the analysis.

After applying these three restrictions, equations (4-7) and (4-8) can be written

$$\bar{u} \frac{\partial \bar{u}}{\partial x} + \bar{v} \frac{\partial \bar{u}}{\partial y} = - \left[ \frac{\partial}{\partial x} (\overline{u'^2}) + \frac{\partial}{\partial y} (\overline{u'v'}) \right] \quad (4-10)$$

$$\bar{u} \frac{\partial \bar{v}}{\partial x} + \bar{v} \frac{\partial \bar{v}}{\partial y} = - \left[ \frac{\partial}{\partial x} (\overline{u'v'}) + \frac{\partial}{\partial y} (\overline{v'^2}) \right] \quad (4-11)$$

Further reduction of (4-10) and (4-11) requires additional information concerning turbulent phenomenon. The presentation of theories regarding this phenomenon and the resulting reduction of terms is left to the literature review. The theories cited in the literature section are viewed with an eye toward their creditability and will be applied to the specific case studied.

## CHAPTER V

## REVIEW OF THE RELATED LITERATURE

Prior to engaging in the specific problem at hand, it appears logical to study the related works of previous investigators. This is done in the hope that physical insights can be gained which will carry over to the present study.

For purposes of clarity, the cited literature will be classified under three general headings. Those three sections will be laminar stability, phenomenological theories and statistical.

## A. Laminar Stability

This subject was touched upon in the introduction. While such studies do provide a good background of information regarding the onset of turbulence, they are not particularly appropriate to this study and will only be briefly summarized here.

There are two approaches utilized in this type of study. The first is the energy method. This method is premised on the belief that the intensity of any fluctuating particle must necessarily decay with time unless some additional energy is supplied to the flow. The second approach is the small perturbation technique. Small perturbation studies have indicated that turbulence originates at a point and then expands in much the same manner that a Mach cone expands in supersonic flow.

The stability studies do not lead to a solution of the equations of motion, and the expressed object of this thesis is the solution of those equations as applied to this mixing region. Thus little in the

way of applicable information could be gained by belaboring this type of approach.

## B. Phenomenological Theories

Due to the amount of material included in this topic, it is subdivided into analytical and experimental work.

### 1. Analytical

The first of the turbulence theories were Reynold's introduction of the "apparent shear" notion and Boussinesq's introduction of the eddy viscosity term. Reynolds reasoned that turbulent flow results in greater pressure losses than laminar flow, therefore, there must be additional stresses involved. Boussinesq attempted to relate apparent shear to the mean velocity profile. He developed the following relationship.

$$\tau_{xy} = -\rho \overline{(u'v')} = \rho \epsilon \frac{d\bar{u}}{dy} \quad (5-1)$$

Equation (5-1) is of the same form as the laminar shear equation. Unlike laminar viscosity ( $\mu$ ), the eddy viscosity was found to be a complex function of local conditions. Thus, the Boussinesq theory is of limited application.

It remained for Prandtl to introduce the first workable phenomenological theory. His theory, now a classic, is the momentum transfer or mixing length theory. His theory, it should be noted, was developed for a turbulent boundary layer and not a turbulent mixing region. Justification for this extension is more properly reserved for the theoretical developments of the following section.

Prandtl<sup>6</sup> postulated a simplified model of momentum transfer for turbulent flow (see Figure 4). He postulated that at a given transverse point ( $y$ ), lumps of fluid will arrive at random intervals. These fluid lumps begin their transverse motion at an arbitrary distance  $L$ , the mixing length, from the point  $y$ . If two lumps originate from opposite sides of  $y$  (at  $y + L$  &  $y - L$ ), they will collide at  $y$ . The ensuing process is a momentum exchange between these lumps and the fluid already at  $y$ . If it is assumed that the lumps maintain their initial mean velocity until the collision, the velocity fluctuation produced by this momentum exchange is the same as the longitudinal fluctuations in the actual flow. Based on these considerations, the continuity equation indicates that the transverse and longitudinal fluctuations will be of the same magnitude.

The difference between the mean time average velocities of the fluid lump arriving from the point ( $y + L$ ) and the fluid already at  $y$  may be mathematically expressed as

$$\Delta \bar{u}_x = \bar{u}(y+L) - \bar{u}(y) \quad (5-2)$$

Shames expressed  $\bar{u}(y + L)$  as a Taylor series about  $y$ . He says that since  $L$  will be small, only two terms of the series need be retained. Thus (5-2) becomes

$$\Delta \bar{u}_x = \left[ \bar{u}(y) + \left( \frac{d\bar{u}}{dy} \right) L \right] - \bar{u}(y) = L \left( \frac{d\bar{u}}{dy} \right) \quad (5-3)$$

A similar expression is written for the velocity difference of the lump arriving from ( $y - L$ ). Shames states that the mean time average of the magnitude of the fluctuating longitudinal velocity component is

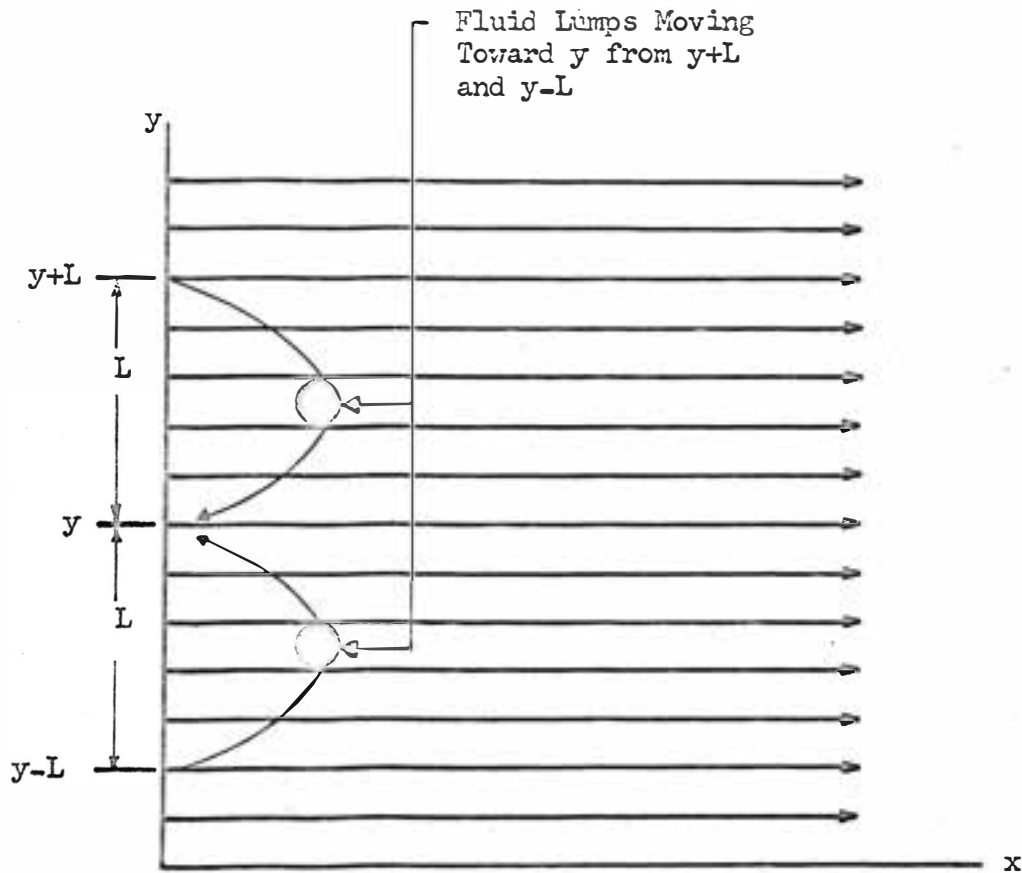


Figure 4. Prandtl's Mixing Concept

the average magnitude of these two velocity differences. This is written as

$$\overline{|u|} = L \left| \frac{du}{dy} \right| \quad (5-4)$$

It was previously stated that  $\overline{|u'|}$  and  $\overline{|v'|}$  are of the same order of magnitude; thus,

$$\overline{|u'|} = c \overline{|v'|} \quad (5-5)$$

Therefore

$$\overline{|u'|v'|} = c L^2 \left( \frac{du}{dy} \right)^2 \quad (5-6)$$

Shames writes the following relation.

$$\overline{(u'v')} = -t \overline{|u'| |v'|} \quad (5-7)$$

where  $t$  represents some fraction. Therefore,

$$\tau_{app} = -\rho \overline{(u'v')} = \rho c t L^2 \left( \frac{du}{dy} \right)^2 \quad (5-8)$$

The importance of Prandtl's mixing length theory lies in the fact that it allows determination of the velocity fluctuations as functions of the local velocity profile (which is relatively easy to determine). Equation (5-8) is a logical consequence of the mixing length theory and will assume significance in the succeeding paragraph.

Fortified with the conclusions of Prandtl's mixing length theory, it is now possible to follow Shames analysis for the reduction of equations (4-10) and (4-11). It is noted again that the order of magnitude analysis applied here was developed for a turbulent boundary layer.

Recall equations (4-10) and (4-11).

$$\bar{u} \frac{\partial \bar{u}}{\partial x} + \bar{v} \frac{\partial \bar{u}}{\partial y} = - \left[ \frac{\partial}{\partial x} (\overline{u'^2}) + \frac{\partial}{\partial y} (\overline{u'v'}) \right] \quad (5-9)$$

$$\bar{u} \frac{\partial \bar{v}}{\partial x} + \bar{v} \frac{\partial \bar{v}}{\partial y} = - \left[ \frac{\partial}{\partial x} (\overline{u'v'}) + \frac{\partial}{\partial y} (\overline{v'^2}) \right] \quad (5-10)$$

The reductive analysis to be applied to (5-9) and (5-10) is an order of magnitude analysis. The purpose of an order of magnitude analysis is the elimination of those terms which probably will not contribute greatly to the results.

Assume that it is possible to assign a scale of measure such that  $u$  (free stream velocity) and  $x$  (downstream dimension) have the same order of magnitude. Define this order of magnitude to be unity, and designate it  $O(1)$ . The magnitudes of the vertical dimensions ( $y$ ) will be much less than  $x$ ; therefore, define it to be  $O(\delta)$  where

$$1 \ll \delta \ll 1$$

substituting these relative magnitudes into the continuity equation (4-3).

$$\frac{\partial \bar{u}}{\partial x} + \frac{\partial \bar{v}}{\partial y} = 0 \quad (5-11)$$

$$\frac{O(1)}{O(1)} + \frac{O(\delta)}{O(\delta)} = 0$$

Obviously (5-11) will be violated unless  $\bar{v} = O(\delta)$ .

Substituting all of this into (5-9) and (5-10) produces

$$\begin{aligned} \bar{u} \frac{\partial \bar{u}}{\partial x} + \bar{v} \frac{\partial \bar{u}}{\partial y} &= - \left[ \frac{\partial}{\partial x} (\overline{u'^2}) + \frac{\partial}{\partial y} (\overline{u'v'}) \right] \\ \alpha) \frac{O(1)}{O(1)} + \alpha(\delta) \frac{O(1)}{O(\delta)} &= - \left[ \frac{O(1)}{O(1)} + \frac{O(1)}{O(\delta)} \right] \end{aligned} \quad (5-12)$$



$$\begin{aligned} \bar{u} \frac{\partial \bar{v}}{\partial x} + \bar{v} \frac{\partial \bar{u}}{\partial y} &= - \left[ \frac{\partial}{\partial x} (\overline{u'v'}) + \frac{\partial}{\partial y} (\overline{v'^2}) \right] \\ \frac{o(1) o(\delta)}{o(1)} + \frac{o(\delta) o(\delta)}{o(\delta)} &= - \left[ \frac{o(\overline{u'v'})}{o(1)} + \frac{o(\overline{v'^2})}{o(\delta)} \right] \end{aligned} \quad (5-13)$$

At this point, examine the fluctuating quantities  $\overline{(u')^2}$ ,  $\overline{(v')^2}$ , and  $\overline{(u'v')}$ . Thus far no statement has been made concerning their absolute magnitude. Note that  $\overline{(u'v')}$  appears in both (5-12) and (5-13). Since  $\overline{(u'v')}$  in (5-12) is taken with respect to  $y$ , which is  $O(\delta)$ , and  $\overline{(u'v')}$  in (5-13) is taken with respect to  $x$ , which is  $O(1)$ , it is reasonable to state that

$$\frac{\partial \overline{(u'v')}}{\partial x} \ll \frac{\partial \overline{(u'v')}}{\partial y}.$$

The only term in (5-12) which requires estimation is  $\overline{(u')^2}$ .

Once again, it is recognized that  $\overline{(u'v')}$  is considered with respect to  $y$  and  $\overline{(u')^2}$  with respect to  $x$ . One can deduce from an analysis similar to equation (5-7) that  $\overline{(u')^2}$  and  $\overline{(u'v')}$  are of a comparable order of magnitude. Thus, it is concluded that

$$\frac{\partial \overline{(u')^2}}{\partial x} \ll \frac{\partial \overline{(u'v')}}{\partial y}.$$

Equation (5-12) is of order unity while (5-13) is of order  $(\delta)$ . Thus, the effects of (5-12) upon the general solution will predominate and (5-13) is neglected. Thus, there is no need to evaluate  $\overline{(v')^2}$  since it does not appear in the equation to be considered (5-12).

Rewrite (5-12) taking note of the fact that  $\overline{(u'v')}$  is now essentially a function of  $y$  only and that the first term on the right hand side is negligible with regard to the remaining terms.

$$\bar{u} \frac{\partial \bar{u}}{\partial x} + \bar{v} \frac{\partial \bar{u}}{\partial y} = - \frac{d}{dy} (\overline{u'v'}) \quad (5-14)$$

Refer back to equation (5-8) and note the effect upon (5-14) if  $L$  is assumed to be invariant with  $y$ . It is seen that the apparent shear term of (5-14) is easily determined as a function of the mean velocity profile and this mixing length. Prandtl assumed that  $L$  would be constant except near a solid boundary. Thus, researchers<sup>8</sup> who have extended Prandtl's boundary layer theory to turbulent mixing regions have hypothesized that

$$L(y) = c \quad (5-15)$$

throughout the mixing zone.

However, Liepmann and Laufer<sup>5</sup> have stated categorically after extensive measurements in free mixing zones that this mixing length is not even approximately constant with  $y$ . This would appear to relegate the mixing length theory to the same status as the eddy viscosity; namely, that of being attractive but unsolvable since it is a function of indeterminable local conditions. This is not the case for two reasons.

The first of these reasons is the reasonable agreement obtained between the actual velocity profile and the theoretical based on the mixing length theory. This agreement is obtained despite the fallacy of the basic assumption.

Secondly, the momentum transfer associated with this theory provides a physical concept which has proven valuable to researchers. Thus, while not providing a wholly contained answer in itself, Prandtl's

theory gives rise to others. The best review of these phenomenological theories is found in either Abramovich<sup>9</sup> or Hinze.<sup>10</sup>

Taylor felt that there was a flaw in Prandtl's mixing length theory. Thus, he postulated a model of his own. His model stated that the shearing stresses are the result of vorticity transfer rather than momentum transfer.

Actually Taylor's theory is based upon the assumption of a mean free path which is analogous to Prandtl's mixing length. As a matter of fact, Taylor's mean free path differs from the mixing length only by a factor of  $\sqrt{2}$ . Furthermore the velocity profiles resulting from each of the theories are nearly identical. Thus, Taylor's theory does not hold any substantial advantages over Prandtl's theory for the purposes of the present study.

Prandtl revamped his theory of turbulence, after experiments had indicated its inherent fallacies. He based his new theory on the assumption of a constant coefficient of turbulent viscosity. He expressed this new theory as

$$\epsilon = \chi \delta (\overline{u_M} - \overline{u_x}) \quad (5-16)$$

Gortler<sup>7</sup> utilized the Boussinesq notion of apparent shear and equations (5-14) and (5-16) to obtain an exact solution for an idealized mixing zone. His solution assumes that there is no initial boundary layer for the two dimensional mixing zone formed by the merging of parallel jets having different velocities.

Gortler postulated a stream function ( $\psi$ ) as a function of some dimensionless distance  $y$ .

$$\psi = \chi U F(\eta) \quad (5-17)$$

where

$$\eta = \delta \frac{y}{x} \quad \& \quad U = \frac{1}{2} (\bar{u}_M + \bar{u}_N) \quad (5-18)$$

where  $\delta$  is an experimental constant.

Applying (5-17) and (5-18) to the definition of the stream function, the following expressions for  $u$  and  $v$  can be written.

$$\frac{u}{U} = \delta F'(\eta) \quad \& \quad \frac{v}{U} = \eta F'(\eta) - F(\eta) \quad (5-19)$$

At this point, Gortler applied (5-16) to Boussinesq's apparent shear idea to determine an expression for  $\overline{(u'v')}$  as a function of the mean velocity profile.

$$\overline{(u'v')} = -\chi B (\bar{u}_M + \bar{u}_N) \quad (5-20)$$

Gortler substituted (5-20) into (5-14) and performed the transformations indicated by (5-18) and (5-19). This resulted in the following differential equation.

$$F'''(\eta) + 2\delta F(\eta) F''(\eta) = 0 \quad (5-21)$$

After making the assumption of asymptotic velocity profiles at  $\eta = \pm \infty$ , he proposed a series solution for  $F(\eta)$ . This series was reduced by writing out the terms for  $F(\eta)$  and each of its first three derivatives. Substituting those into (5-21) and equating coefficients of like powers, he was able to evaluate the first few terms and truncate the series.

Assuming this truncated series to be sufficiently accurate, the following expression for the velocity profile is obtained

$$\frac{\bar{u}}{U} = 1 + \frac{2}{\pi} \left( \frac{u_m - u_H}{u_m + u_H} \right) \int_0^{\eta} e^{-z^2} dz \quad (5-22)$$

It should be noted that Gortler's solution assumes straight-line expansion of the mixing zone. This assumption is based on empirical work done by Abramovich on models similar to the one considered by Gortler. Abramovich developed this relationship for the growth of the mixing region.

$$b = cX \left( \frac{1-m}{1+m} \right) \quad (5-26)$$

where  $m$  is the ratio of the free stream velocities  $\bar{u}_m$  and  $\bar{u}_H$ .

Another noteworthy development in the realm of phenomenological turbulence theories is the similarity theory by von Karman.<sup>5</sup> By a procedure analogous to that utilized by Prandtl, von Karman postulated a relationship for apparent shear

$$\tau_{app} = K^2 \rho \frac{\left( \frac{\partial \bar{u}}{\partial y} \right)^4}{\left( \frac{\partial^2 \bar{u}}{\partial y^2} \right)^2} \quad (5-27)$$

where  $K^2$  is a constant analogous to the exchange coefficient.

The similarity parameter is susceptible to gross inaccuracies near an inflection point of the velocity profile. Therefore, it is not particularly amenable to mixing region studies and will not be discussed further here.

Two sets of researchers have developed integral type solutions to the two dimensional mixing region in which the initial boundary

layer is considered. The analyses were done by Torda and Stillwell<sup>6</sup> and Liepmann and Laufer. The solutions are based on a simultaneous solution of integral forms of the energy and momentum equations. This solution allows the prediction of the growth of the mixing region. The only prerequisite is the experimental velocity profile.

In summary, the theories reviewed here are the foremost analytical developments in the field of turbulent mixing regions. The analysis to be presented for the present study is predicated upon Prandtl's mixing length theory. The actual solution is of the momentum integral type mentioned. An exact solution will not be attempted, rather an effort will be made to correlate Gortler's work. Before continuing with that analysis, a presentation of prior experimental work is in order.

## 2. Experimental

Abramovich cites the works of several researchers who have contributed experimental data in this field. It is emphasized at the outset that the cases Abramovich studied did not include initial boundary layer effects. Thus, the results will not be directly applicable to the present study.

One interesting conclusion that Abramovich draws from experimental data is the universality of the dimensionless velocity profile. Universality means that the dimensionless velocity profile remains identical in the downstream ( $x$ ) direction where the velocity is non-dimensionalized by dividing local velocity by the velocity at the jet axis. Forthmann<sup>8</sup> noted this universality for submerged jets. A

submerged jet is characterized by a moving stream entering a zero velocity environment. This universality of velocity profiles was extended by Weinstein<sup>8</sup> to the case of two merging streams at unequal velocities. This observation becomes important in view of a subsequent study done by Liepmann and Laufer. They utilized a hot-wire anemometer to measure the turbulent components in a mixing region formed by a jet expanding from a rectangular (60" x 7.5") contraction into a still atmosphere. In other words, they studied the effects of a two dimensional submerged jet in which there was an initial boundary layer. The boundary layer was very thin and laminar at the exit of the contraction.

Liepmann and Laufer noted that the mixing region was laminar for a short distance downstream. The laminar region was followed by a transitional region and then a fully developed turbulent region. The exact delineations between the transitional and the turbulent region is not easily determined. It was noted, however, that the laminar region was fairly short. It was also noted that once fully turbulent flow was attained, the velocity profiles demonstrated the universality noted by those researchers whose models did not include initial boundary layers. Also the mixing region boundaries in the turbulent region were noted to be straight line expansions. This also agrees with the conclusions noted by Abramovich.

The next logical step is the study of a mixing region formed by the merging of two parallel streams at unequal velocities in which initial boundary layer effects are to be considered. Just such a model

was studied by Torda and Stillwell. However, they used pressure probes to determine velocities. Thus, they could not measure any of the turbulent components. They assumed that the mixing region is only an extension of the boundary layer. Thus, Torda and Stillwell defined the mixing region boundaries to be the locus of points at which the velocity reached 95% of its free stream value. They did not, as a matter of fact, could not, determine if this point at which  $\frac{\partial u}{\partial y}$  became essentially zero was coincident with the point at which the turbulence intensity became zero. It appears that the work of Torda and Stillwell leaves the problem of merging parallel streams of unequal velocities unresolved.

Torda and Stillwell were primarily concerned with the description of the mean velocity profile. This was the only quantity they needed to determine so that they might simultaneously solve their integral equations. They postulated a velocity profile which was a function of the dimensionless minimum velocity. They measured the velocity profiles and found reasonable correlation with the predicted profile. They found that the minimum velocity recovered faster than they predicted. They also predicted, on the basis of momentum considerations, a slight contraction of the mixing boundaries at the trailing edge of the splitter plate. This contraction was verified in the measurements. They did not specify the thickness of the splitter plate. However, it will be assumed in the present study that a thin plate will not produce a noticeable contraction.

Several researchers have measured and plotted the turbulent



components. They are usually plotted as  $\frac{\overline{(u')^2}}{u_\infty^2}$ ,  $\frac{\overline{(v')^2}}{u_\infty^2}$  and  $\frac{\overline{(u'v')}}{u_\infty^2}$  where  $u_\infty$  is the free stream velocity. One can obtain a grasp of the relative magnitude of each of the terms when they are plotted in this way. Schlichting<sup>7</sup> has published data which shows  $\overline{|u'|}$  and  $\overline{|v'|}$  to be approximately equal within a boundary layer. This is in accordance with the mixing length theory. Abramovich noted good agreement between the Gortler and measured velocity profiles. This is to be expected for the models he studied. Also, he has shown that  $\overline{|u'|}$  and  $\overline{|v'|}$  are of the same order of magnitude in the two dimensional mixing zone for which there is no initial boundary layer. He cites both the submerged jet and parallel, unequal streams cases. In each type of mixing zone, the pattern is the same. That is  $\overline{|u'|}$ ,  $\overline{|v'|}$  and  $\overline{(u'v')}$  reach their maximum values near the center of the mixing zone and approach zero at the edges. It is noted that  $\overline{|u'|}$  remains slightly larger than  $\overline{|v'|}$  throughout the region.

Liepmann and Laufer, noted reasonably good agreement with Gortler's theoretical velocity profile. They also plotted the turbulent components  $\frac{\overline{(u')^2}}{u_\infty^2}$ ,  $\frac{\overline{(v')^2}}{u_\infty^2}$ ,  $\frac{\overline{(u'v')}}{u_\infty^2}$  and noted the same trends as were observed for the zero boundary layer cases. The components were plotted for various downstream dimensions (see Figure 5). The  $\overline{|u'|}$  was found to be considerably higher across the mixing zone than  $\overline{|v'|}$ . Both reach maximums near the center of the mixing zone. The measured  $\overline{(u'v')}$  components are smaller than the values expected from apparent shear theories. This is due in part to the deviations between the Gortler and actual velocity profiles. Further, the theoretical calcula-

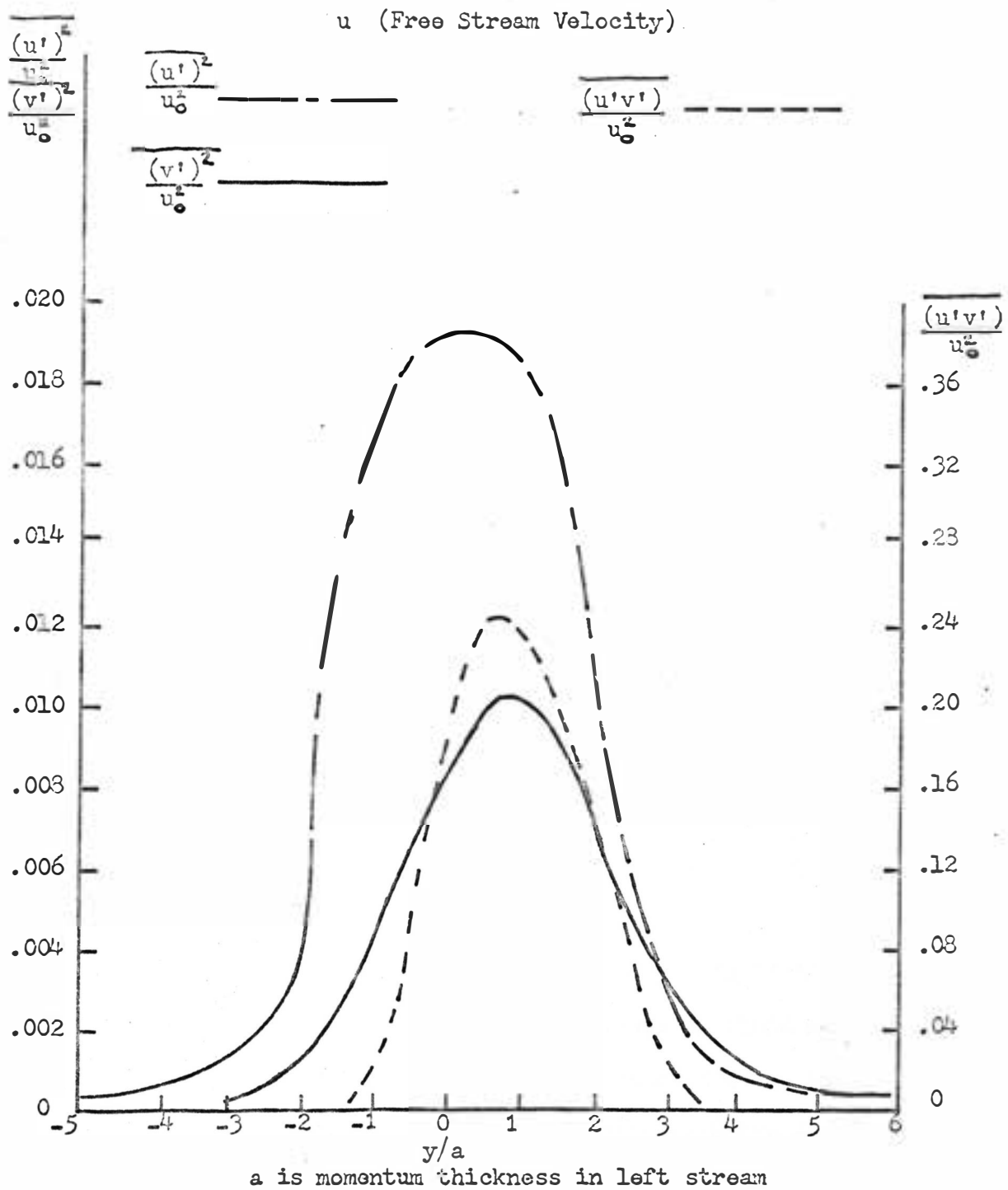


Figure 5. Typical Apparent Shear, Normal and Transverse Turbulence Component Profiles

tion assumes turbulent flow across the entire width of the mixing zone. Good agreement was obtained between the apparent shears calculated from the actual profiles and the measured shears.

A final calculation was made by Liepmann and Laufer to determine the mixing length and the constant exchange coefficient distributions throughout the mixing region. These quantities were calculated from the measured shear values and the actual velocity profile. The plots show that the mixing length and exchange coefficient are anything but constant across the mixing zone.

In conclusion, all researchers, whether their models included or did not include initial boundary layers, produced the same information concerning the turbulent components. These findings are represented in Figure 5. Further these researchers whose models did have initial boundary thicknesses found Görtler's theoretical profile to be reasonably valid. Torda and Stillwell, however, felt that it was necessary to account for the  $x$ -dependency of the velocity profile by introducing a dimensionless minimum velocity.

### C. Statistical Theories

The first of the statistical theories was in 1935 by G. I. Taylor.<sup>5</sup> He crystallized some early concepts of fluid motion and introduced the idea of correlation between velocities at two points as one of the quantities needed to describe turbulence. Since Taylor, work has centered around two aims with regard to statistical theories of turbulence.

The first of these aims is a solution of equation (5-14) through

application of statistical theories. This approach has not been very fruitful. For, as noted by Hinze, (5-14) has a non-linear term. Thus, researchers have been stymied by a situation in which there always exists one more unknown than there are equations. The analysis hinges on the ability of the researcher to truncate the number of equations at a point where a reasonable accuracy is obtained.

The second goal of statistical researchers is the study of the decay of eddies. Batchelor<sup>10</sup> deduced that the small eddies will derive their energy from the large eddies in high inertia turbulence. The small eddies are said to be in statistical equilibrium. That is, the amount of energy transferred is significantly greater than the energy change of the small eddies. On the basis of these postulates a hypothesis of universal equilibrium has been developed. This hypothesis states that the motion associated with the small eddies is uniquely determined by the imparted energy from the large eddies and the viscous dissipation. If this hypothesis is valid, it will infer that the motions associated with small eddies have a characteristic statistical form. However, sufficient experimental verification has not been provided; thus, the hypothesis lacks the necessary basis for wide acceptance.

Batchelor cites experimental data which attempts to empirically develop an energy decay law. It was found that the decay of turbulence created by a grid is actually divided into three separate regions. In the initial region, the effects of large eddy decay are the predominate factors. The initial region is followed by a transitional region

and then a region in which the small eddy decay effects predominate.

Additional experimental work has been done by Townsend.<sup>10</sup> He used a variety of grid geometries to trip the flow to turbulence. His results indicate that the turbulence in all cases quickly settles to a statistical state in which the distribution of about 80% of the total energy, that part contained by the small eddies, is nearly independent of the grid geometries. This would appear to substantiate the previously noted hypothesis of universal equilibrium. However, Townsend did not feel that any general theorems should be deduced from his results.

It seems appropriate to mention, at this time, the application of this discussion of eddy decay to the present case. It is inferred from this discussion that the large eddies will be formed in the region immediately downstream of the end of the splitter plate (see Figure 3). As the flow travels further downstream, the large eddies in the center of the mixing zone will feed the smaller ones on the edges. Eventually the large eddies will be broken down and the small eddies will remain. At this point (i.e.,  $x=10^4$ ), the velocity profile will dampen out and the minimum velocity should be recovered to a value nearly equal to the free stream velocity.

## CHAPTER VI

## ANALYTICAL CONSIDERATIONS

Recall equation (5-14) which is the Navier-Stokes equation of motion reduced to a form applicable to turbulent boundary layers.

Recall that this reduction was achieved through the implementation of Prandtl's mixing length theory and an order of magnitude analysis.

$$\bar{u} \frac{\partial \bar{u}}{\partial x} + \bar{v} \frac{\partial \bar{u}}{\partial y} = - \frac{\partial}{\partial y} (\overline{u'v'}) \quad (5-14)$$

Prior to extending (5-14) to the present case, it is felt that justification should be presented. Examine first the assumption that  $\overline{u'u'} = 0$ . This is based on Prandtl's theory and appears to have been verified in other studies. However, theoretical assumptions such as this require specific experimental verification when applied to definite cases. While Liepmann and Laufer have verified this for their purposes, it is felt that the establishment of this relationship is fundamental to this analysis. Liepmann and Laufer dealt with the case of a very thin, laminar boundary layer upstream of the nozzle exit. It is reasonable to assume that the boundary formed in the present study by the screens will be thick and possess at least a degree of turbulence.

Examine also the assumption  $\frac{\partial}{\partial x} (\overline{u'})^2 \ll \frac{\partial}{\partial y} (\overline{u'v'})$ .

Recall that statistical analyses indicate that the small eddies lose their energy by viscous dissipation. Since, obviously, the majority of the viscous dissipation takes place at the edges of the mixing region, one must conclude that the small eddies will be found at the

edge. The larger eddies which replenish the small eddies, will be found near the center of the mixing region. Thus, one can anticipate that there will be a fairly wide range of turbulent intensities across the mixing region. This range of intensity should result in a substantial  $\frac{\partial}{\partial y}(u'v')$  quantity. On the other hand, due to the redistributive effect of eddy energy, the decay of eddies in the downstream direction should not be too severe. An exception may occur at the centerline where extremely high fluctuations should damp out fairly quickly. In an event, the longitudinal change of intensity should not be so severe as the transverse change.

Experimental evidence bolsters this analysis. Work done by Batchelor and Liepmann and Laufer are cited as cases in point. However, as stated before, Batchelor's study was a case of free and isotropic turbulence and Liepmann and Laufer did not have a thick, turbulent boundary layer upstream of the mixing region. Thus, while this assumption of  $\frac{\partial}{\partial x}(u')^2 \ll \frac{\partial}{\partial y}(u'v')$  appears valid for the present study, it will be checked experimentally.

Assume for the present time that the assumptions upon which (5-14) is predicated are justifiable; and turn the emphasis to the solution of equation (5-14).

Several approaches have been attempted by various researchers. Among these approaches are the exact, statistical, and integral. An exact solution has been developed by Gortler for the idealized case studied by Abramovich. Gortler's solution has been corroborated by several researchers<sup>11</sup> whose models included upstream boundary layers.

Thus, there will be no original exact solution presented here; rather an attempt will be made to match the Gortler profile with the results. The statistical solution, as was mentioned previously, becomes an unwieldy set of simultaneous equations. Therefore, the approach selected for this study is the integral approach.

The integral approach was tried by both Liepmann and Laufer and Forda and St. Alwell. Their analyses involved the simultaneous solution of integral forms of the motion and energy equations. This procedure was followed because they were hesitant to make restrictive assumptions concerning the expansion of the mixing zone. For the present study, a restricted case will be attempted. It is felt that information now exists which allows the researcher to make predictions concerning the growth of the mixing region. Whether these predictions are valid in a new environment is subject to experimental proof.

Integrate equation (5-14) between the mixing zone boundaries which are  $a(x)$  and  $b(x)$ .

$$\int_a^b \bar{u} \frac{\partial \bar{u}}{\partial x} dy + \int_a^b \bar{v} \frac{\partial \bar{v}}{\partial y} dy = - \int_a^b \frac{d}{dy} (\bar{u} \bar{v}) dy \quad (6-1)$$

From the continuity equation (4-1), it is possible to write

$$\int_a^b \bar{v} \frac{\partial \bar{v}}{\partial y} dy = - \int_a^b \left( \int_0^y \frac{\partial \bar{u}}{\partial x} dy \right) \frac{\partial \bar{u}}{\partial y} dy \quad (6-2)$$

Integrate by parts to obtain

$$\int_a^b \bar{v} \frac{\partial \bar{v}}{\partial y} dy = - \bar{u}_0 \int_0^b \frac{\partial \bar{u}}{\partial x} dy + \bar{u}_a \int_0^a \frac{\partial \bar{u}}{\partial x} dy + \int_a^b \bar{u} \frac{\partial \bar{u}}{\partial x} dy \quad (6-3)$$

where  $\bar{u}_0$  and  $\bar{u}_a$  represent the mean velocity at each of the mixing



boundaries.

Substitute equation (6-3) into (6-1), noting that at the mixing boundaries, the turbulence intensity should be negligible.

$$\int_a^b \bar{u} \frac{\partial \bar{u}}{\partial x} dy + \left[ \bar{u} \frac{\partial \bar{u}}{\partial x} \right]_a^b - \bar{u}_b \int_a^b \frac{\partial \bar{u}}{\partial x} dy + \bar{u}_a \int_0^a \frac{\partial \bar{u}}{\partial x} dy = 0 \quad (6-4)$$

Combining terms in (6-4) yields

$$\int_a^b \frac{\partial}{\partial x} (\bar{u}^2 - \bar{u}_b \bar{u} - \bar{u}_a \bar{u}) dy + \bar{u}_b \int_a^0 \frac{\partial \bar{u}}{\partial x} dy + \bar{u}_a \int_0^b \frac{\partial \bar{u}}{\partial x} dy = 0 \quad (6-5)$$

Applying Leibnitz rule<sup>12</sup> to each of the integrals in (6-5)

successively yields

$$\frac{d}{dx} \int_a^b \bar{u} (\bar{u} - \bar{u}_b - \bar{u}_a) dy = \bar{u} [\bar{u} - \bar{u}_b - \bar{u}_a] \left( \frac{dy}{dx} \right)_a^b + \int_a^b \frac{\partial}{\partial x} [\bar{u} (\bar{u} - \bar{u}_b - \bar{u}_a)] dy \quad (6-6)$$

$$\frac{d}{dx} \int_a^0 (\bar{u}_b \bar{u}) dy = (\bar{u}_b \bar{u}) \left( \frac{dy}{dx} \right)_a^0 + \int_a^0 \frac{\partial}{\partial x} (\bar{u}_b \bar{u}) dy \quad (6-7)$$

$$\frac{d}{dx} \int_0^b (\bar{u}_a \bar{u}) dy = (\bar{u}_a \bar{u}) \left( \frac{dy}{dx} \right)_0^b + \int_0^b \frac{\partial}{\partial x} (\bar{u}_a \bar{u}) dy \quad (6-8)$$

After evaluation at the indicated limits, equations (6-6),

(6-7) and (6-8) are substituted into (6-5). After simplification this yields

$$\frac{d}{dx} \int_a^b (\bar{u}^2 - \bar{u}_b \bar{u} - \bar{u}_a \bar{u}) dy + \frac{d}{dx} \int_a^0 (\bar{u}_b \bar{u}) dy + \frac{d}{dx} \int_0^b (\bar{u}_a \bar{u}) dy = 0 \quad (6-9)$$

At this point, define the ratio of the free stream velocities at the edges of the mixing region as  $m$ . Also assume that for the present study, the ratio of the mixing boundaries is a constant. This is expressed as

$$b = ca \quad (6-10)$$

Note that implicit to this assumption is the inference that each of the boundaries grows linearly with the downstream dimension ( $x$ ). It is unlikely that curved boundaries would maintain a constant ratio. The assumption of linearity is established by Abramovich for his model. He postulated that  $|v'|$  is the component which causes the mixing region to grow. Then he demonstrated through Prandtl's mixing length theory that this growth should be linear. Further verification can be drawn from the results of Liepmann and Laufer. They noted linearity once the mixing region became fully developed turbulent flow. In the present study, a degree of turbulence is created by the screen. This should shorten the initial and transitional periods and improve the assumption of linearity.

Rearranging equation (6-9) on the basis of the preceding discussion yields an equation containing only  $m$ ,  $\bar{u}$ ,  $\bar{u}_a$ ,  $a$ , and  $c$ .

$$\int_a^{ac} (\bar{u}^2 - \bar{u}_a \bar{u} - m \bar{u}_a \bar{u}) dy + \int_a^0 (m \bar{u}_a \bar{u}) dy + \int_0^{ac} (\bar{u}_a \bar{u}) dy = K \quad (6-11)$$

where  $K$  is a constant of integration.

At this point, it is necessary to substitute an appropriate velocity profile into (6-11) so that  $(a)$  may be determined as a

function of  $x$ . Torda and Stillwell have found that an appropriate form for the velocity profile is

$$\frac{u}{u_a} = \alpha f(\eta/a) \quad (6-12)$$

In this profile  $\alpha$  is a function of  $x$  and is the dimensionless minimum velocity. Thus, this profile will account for frictional effects due to severe gradients. It should be noted that the distance ( $a$ ) is the distance to one of the free streams. That is, at ( $a$ ) the average velocity and the turbulence components approach asymptotically their free stream values. This is in accordance with the supposition made previously that the mixing zone action is analagous to the boundary layer action. This assumption should be subjected to experimental verification to determine if in fact the points at which  $\frac{d\bar{u}}{dy} \approx 0$  and  $(u')^2 \approx 0$  are coincident. If they do not coincide, it will be necessary to alter the form of the velocity profile.

Defining

$$\eta = y/a \quad (6-13)$$

and substituting (6-13) and (6-12) into (6-11) yields

$$a \int_1^c [\bar{u}_a^2 \alpha^2 f^2(\eta) - m \bar{u}_a^2 \alpha f(\eta) - \bar{u}_a^2 \alpha f(\eta)] d\eta + \int_0^c m \bar{u}_a^2 \alpha f(\eta) d\eta + a \int_0^c \bar{u}_a^2 \alpha f(\eta) d\eta = K \quad (6-14)$$

The constant  $c$  must be experimentally determined. Abramovich found it to be about 0.25 for his studies. After substituting for  $\bar{u}_a$  and  $m$

$$a H(\alpha) = K \quad (6-15)$$

where  $H(\alpha)$  is the value of the integrals of (6-14).

The constant of integration is to be evaluated at the trailing edge of the splitter plate ( $x=0$ ). At this point, the thickness ( $\alpha$ ) can be determined either by measurement or calculation through an appropriate boundary layer build-up equation. In this case, because a screen was used, it will be necessary to measure the thickness.  $H(\alpha)$  can also be evaluated at  $x=0$  by experimental information.

A similar solution can be provided for the special case in which the two streams have equal velocities. The same assumptions apply to this case as the unequal flow with an additional restriction of symmetry, ( $c=1$ ).

Recognizing that  $m=1$ , it is possible to write

$$\int_0^{\alpha} (\bar{u}^2 - \bar{u} \bar{u}_a) d\eta = M \quad (6-16)$$

Substitution of equation (6-12) into (6-16) yields

$$\alpha \int_0^1 [\bar{u}_a^2 \lambda^2 f^2(\eta) - \bar{u}_a^2 \lambda f'(\eta)] d\eta = M \quad (6-17)$$

This leads to

$$\alpha G(\alpha) = M \quad (6-18)$$

where  $G(\alpha)$  is the value of the integral of (6-17) and where  $M$  like  $K$  is to be evaluated at the trailing edge of the splitter plate.

This completes the analytical considerations. The solutions indicated for the unequal and equal flows require only a properly defined velocity profile. It is hoped that the experimental data can be analyzed to produce such a profile.

Several assumptions were made during the course of this

analysis and require experimental verification. Two assumptions were made during the process of reducing (4-2) to (5-14); those two have been emphasized previously. Two additional assumptions were made in the completion of the integral solution and require experimental proof. Those assumptions are: (1) the mixing boundaries expand linearly and (2)  $\frac{\partial \bar{u}}{\partial y} \approx 0$  and  $(\bar{u}')^2 \approx 0$  at the same point. Finally, of course, it will be necessary to describe a velocity profile in the form  $\frac{\bar{u}}{u_a} = \alpha f(\eta)$ .

## CHAPTER VII

## RESULTS AND DISCUSSION

A brief note discussing the procedure utilized in gathering and analyzing the experimental data is presented in this section. It is presented for the sole purpose of relating it to the discussion of results.

A total of five different flow situations were studied. Three equal flow cases were studied at 39, 61 and 113 feet per second. Two unequal flow cases were studied. In one case, the velocities were 113 and 51 feet per second. In the other case, the velocities were 67 and 43 feet per second. The measurements for the 39 and 113 feet per second runs were taken in the channel depicted on the right in Figure 3. The 61 feet per second reading was taken in the left hand channel. The hot-wire anemometer probe was traversed through the calibrated lower slot for the  $x=0$ , 1, and 2 settings, and the upper slot for  $x=5$  and 10. The readings were concentrated near the center-line ( $y=0$ ) since it was felt this would be the area of maximum change.

The information was analyzed on an IBM 1620 computer, after the appropriate program was supplied. The equations utilized were based on a truncated series method presented in the Flow Corporation booklet "Hot Wire Anemometer Theory and Instructions".<sup>13</sup> A short method for calculating the turbulent components has been discussed by Gessner.<sup>14</sup> His method is highly restrictive in that it cannot be applied to probes in which the wires are not perpendicular, and for which the cooling time constant is not unity. In the course of exper-

imentation, it was found that these two restrictions could be relaxed. A subsequent paper was submitted jointly by Prof. B. E. Eno, Mr. O. T. Sessions and this author<sup>15</sup> to the ASME Journal of Applied Mechanics. A summary of this paper is found in Appendix B.

Prior to engaging in an analysis of Figures 6 through 17, certain reservations should be stated concerning the data. The turbulence intensity throughout the region of study was extremely high. It was often as high as 40% in the region near  $y=0$ . The recommended upper limit for the hot-wire anemometer unit is 15%. Beyond this limit, the reproducibility of the unit (due to the time lag of its circuitry) is limited. There are two primary sources of excessive turbulence in this study.

It is noted that the duct itself may inherently add to the turbulence intensity. The turbulence intensity throughout what is considered the free stream is about 7%. This is extremely high compared to works of other researchers. They maintained intensities of less than 1% in the free stream. This may be attributable to the construction of the duct.

The duct is made of 1/16" sheet metal and as such is capable of pulsating with the fluid. Thus it serves to magnify rather than restrict the fluctuations. Another indication that the duct may be introducing error is the rise in turbulence level at  $x=5$  and 10. Reexamination of previously stated theories of decay makes this observation appear incongruous. This incongruity is interpreted to mean that the laminar flow energy is tripped into turbulence. The

most obvious means by which such a transfer could occur is a wall disturbance. However, no physical obstructions are present near the cited points. Thus the mechanism of energy transfer is unknown.

The screens which were placed in the flow for the purpose of thickening the boundary also induced turbulence into the flow. The screens were placed about 15" upstream of the trailing edge. At this distance, they fulfill the criterion of J. A. Brighton<sup>16</sup> concerning distance to be allotted for damping effects to take place. Brighton has empirically found that a distance equal to 1000 times the wire diameter should be allotted in the downstream direction. This will insure a turbulent velocity profile of the same structure as found in a natural boundary layer. The L/D ratios in the present study vary between 833 (at  $x=0$ ) and 1400 (at  $x=10"$ ).

A type of corrective action which can be applied when turbulent intensity exceeds 15% is the addition of a linearizer to the anemometer unit. By graduating the responses the linearizer can alleviate some of the high intensity error. However, the usefulness of the linearizer has been questioned by two researchers, Parthasarathy and Tritton.<sup>17</sup> They concluded that for the range of turbulence they encountered (less than 25%), the linearizer was not particularly advantageous. They felt that the added accuracy was not warranted by the added cost and complexity.

With these reservations in mind, refer to the figures of Appendix A in the hope that indicative rather than conclusive results can be seen. The discussion of these figures is divided into two



areas. Those areas are: (1) developmental assumptions (those assumptions utilized in reducing (4-2) to (5-14)); and (2) procedural assumptions (those assumptions necessary to the completion of the integral solution of Chapter V).

#### A. Developmental assumptions

Recall that the first subject of experimental proof was the assumption that  $|u'|$  and  $|v'|$  are of the same order of magnitude. For this information, refer to Figure 6. Note that  $(v')^2$  is about 1.1/2 to 2 times as large as  $(u')^2$  throughout the region considered (the larger ratios occur at the edges). This means that the ratio between  $|v'|$  and  $|u'|$  in the region near  $y=0$  is about 1.2. Thus, it appears that this assumption has been reasonably verified.

One unique fact was noted in Figure 6. Recall that all other researchers had found  $|u'|$  greater than  $|v'|$ . This was not true in the present study. The author is unable to rationalize this contradiction of previous data. It should be noted that the wire cooling constant was about 2.2 for each of the wires used. The Flow Corporation booklet states that this constant should approach unity. The quantity  $|v'|$  is proportional to the cooling constant. Thus, this may serve as a mathematical explanation for  $|v'|$  being greater than  $|u'|$ . It does not explain the physical situation.

The second assumption made in reducing equation (4-2) to equation (5-14) was that  $\frac{\partial(u')^2}{\partial x} < \frac{\partial(u'v')}{\partial y}$ . The experimental proof of this assumption is contained in Figures 7 through 16. For each of the three equal velocity and two unequal velocity cases which

were studied two graphs are presented. One graph shows the change of  $\overline{(u'v')}$  across the transverse width. Note that these transverse  $u_a$  profiles are plotted at each of the downstream (x) positions studied.

The second graph pertaining to a given flow case shows the change of  $\overline{(u')}$  throughout the downstream (x) positions.

Selecting the case in which  $u_a = 113$  feet per second and  $u_1 = 51$  feet per second (Figures 13 and 14), some interesting observations can be made. The curves, though irregular, are smooth and continuous. Thus, the establishment of the magnitude of change of each of the quantities should constitute reasonable indication of the magnitude of the gradients. The gradient must be studied between the edges of the mixing zone. However, it is impossible to precisely define the edges of the mixing region from the data. Thus, it is necessary to discuss the anticipated mixing region near  $y=0$ . It is seen that  $\overline{(u'v')}$  changes by a factor of about eight in the region ( $|y| \leq .5$ ). For a comparable distance in x, the change amounts to a factor of 1.4. Based on this, it becomes apparent that  $\frac{\partial}{\partial y} \overline{(u'v')}$  is greater than  $\frac{\partial}{\partial x} \overline{(u')^2}$ . Whether the difference in these terms is in fact an order of magnitude is certainly questionable. However, as was stated before, the attempt here is to demonstrate trends rather than define facts. The same trends are noticed in all the other cases studied.

#### B. Procedural assumptions

The final objective of this thesis was the solution of equation (5-14) by a momentum integral technique. Recall that the

integration hinged on three presumptions which were to be satisfied experimentally. First it was necessary to demonstrate that the boundaries of the mixing zone were linear. However, the screen induced turbulence was such that it obliterated the mixing region delineations and prevented formation of conclusions regarding these boundaries.

A second subject of experimental analysis was the demonstration of the fact the points at which  $u \approx 0$  and  $(u')^2 \approx 0$  are coincident. Thus, it was assumed that there would be a free stream. In this free stream, the velocity should be approximately constant in the transverse ( $y$ ) direction. Also in the free stream, the mixing and screen turbulence should have died out. It was impossible to substantiate the assumption of coincidence. The turbulence intensity was highest at  $y = \pm 2.0$  and the velocity profile never did appear to flatten out.

The final subject of experimentation was the description of an accurate velocity profile in the form of equation (6-12). This could not be done because, as was noted above, no free stream velocity could be detected.

Figure 17 is the author's attempt to correlate the exact solution by Gortler and the measured velocity profile. The degree of correlation was not expected to be high in the immediate ( $x=0, 1, 2$ ) region downstream of the trailing edge of the splitter plate. It was hoped that farther downstream ( $x=5, 10$ ) the mixing region would spread to the extent that its effects would predominate over the screen effects. It can be seen that the final locations exhibit the highest correlation, but the flow is retarded greater than predicted by

Gortler's solution.

One final fact is noted in Figures 6 through 17. The values of  $\langle u'v' \rangle$  decrease from  $y=0$  to  $y=\pm 0.5$ , and increase to  $y=\pm 2.0$ . While one would expect an initial decrease, the increase from  $\pm 0.5$  to  $\pm 2.0$  is difficult to reconcile. Two possible explanations arise here.

First, the turbulence created by the screen might be of magnitude and breadth such that it completely filled the duct. Thus, a free stream condition was never reached. In that case, all the measured turbulent components should be high. A wider channel would be necessary to determine the transverse point at which the fluctuations died out.

A second possibility is that the situation may not be two-dimensional at all. The bulk of the mixing zone studies are conducted on submerged jets to insure the existence of a relatively unlimited quantity of fluid which can be entrained into the retarded region to supply additional momentum. In a duct, particularly the duct used in the present study, a definite limit is set on the available fluid. Thus, it is extremely difficult to maintain two-dimensional flow.

Tracy<sup>17</sup> has presented a study which shows the three-dimensional nature of turbulent duct flow. His data indicates that  $\langle u' \rangle^2$ ,  $\langle v' \rangle^2$  and  $\langle w' \rangle^2$  are approximately equal near the center of the channel. Also  $\langle u'v' \rangle$ ,  $\langle u'w' \rangle$  and  $\langle v'w' \rangle$  are approximately equal in this area. He also noted secondary velocity (circulation) vectors originating in

the corners and spreading toward the center.

Based on Tracy's information, the assumption of two-dimensionality and the order of magnitude analysis seem shaky indeed. The true picture might well be a three-dimensional one in which the energy exchanges include  $\overline{(w')^2}$ ,  $\overline{(u'w')}$  and  $\overline{(v'w')}$ . These terms may account for the strange energy distribution that was noted. However, Hinze has stated that an analysis of a three-dimensional situation requires the determination of the triple velocity correlation  $\overline{(u'v'w')}$ . To this author's knowledge, no measuring device is capable of determining this quantity.

## CHAPTER VIII

## CONCLUSIONS AND RECOMMENDATIONS

It was found that accurate measurements are nearly impossible with the present apparatus. This is due to the extremely high level of turbulence. Two courses of action were mentioned and they were: (1) add a linearizer circuit to the measuring units to improve measuring capacity, and (2) attempt to eliminate or at least control the extraneous turbulence. It is felt that the extraneous turbulence can be attributed to the boundary layer thickening screens and the 1/16" sheet metal used in the duct. It is felt that the latter course of action is more appropriate here.

It was assumed in Chapter III that the mixing zone would be of a two-dimensional nature. In the last analysis, the solution turns on this assumption. Experiment<sup>18</sup> has shown there are indeed some three-dimensional effects present in any duct flow. These three-dimensional effects will probably become significant in the present duct which has an aspect ratio (width to depth) of unity. It is suggested that a minimum aspect ratio of five to one is necessary to sustain two-dimensional flow.

Finally, it appears that the situation studied was a complex combination of a three-dimensional duct, screens, and a mixing zone. It is somewhat open to question as to whether the mixing action was a major or minor contribution to the observed turbulence.

It was possible to conclude that  $\overline{|u'|}$  and  $\overline{|v'|}$  are of the same order of magnitude. It was inferred from the data that

$\frac{\partial (u')^2}{\partial x} \ll \frac{\partial (u'v')}{\partial y}$ . This inference loses some of its impact in light of the information concerning three-dimensionality.

It was impossible to define free stream velocities or mixing boundaries from the data. It is highly dubious that a high degree of correlation would have resulted even if this experimental information could have been determined and substituted into the integral solutions. The assumptions upon which the analysis hinge now appear to be naive.

This author doubts that there is sufficient mathematics available to the engineer to resolve the complex combination of parameters prevalent in the present duct. It appears that the task will now become that of improving the test facility so that the necessary restrictions may be reasonably applied to it.

## BIBLIOGRAPHY

- (1) Shames, I. H., Mechanics of Fluids, McGraw-Hill Book Company, Inc., New York, New York, 1959.
- (2) Iverson, R. A., "The Design of an Apparatus for Investigating Mixing of Two Parallel Air Streams and Analysis of Half Jet Phenomenon", M.S. Thesis, South Dakota State University, 1964.
- (3) Goel, T. C., "Turbulent Mixing and Heat Exchange in a Parallel Stream of Air", M.S. Thesis, South Dakota State University, 1965.
- (4) Hunt, J. N., Incompressible Fluid Dynamics, John Wiley and Sons, Inc., New York, New York, 1964.
- (5) Liepmann, H. W. and Laufer, J., "Investigations in Free Turbulent Mixing", N.A.C.A., TN 1257, August, 1947.
- (6) Torda, T. P. and Stillwell, H.S., "Analytical and Experimental Investigations of Incompressible and Compressible Mixing of Streams and Jets", WADC Technical Report 55347, 1956.
- (7) Schlichting, H., Boundary Layer Theory, McGraw-Hill Book Company, Inc., New York, New York, 1959.
- (8) Abramovich, G. N., The Theory of Turbulent Jets, M.I.T. Press, Massachusetts Institute of Technology, Cambridge, Massachusetts, 1963.
- (9) Hinze, J. O., Turbulence, McGraw-Hill Book Company, Inc., New York, New York, 1959.
- (10) Batchelor, G. K., The Theory of Homogeneous Turbulence, University Press, Cambridge, England, 1953.
- (11) Chu, W. T., "Velocity Profiles in the Half-Jet Mixing Region of Turbulent Jets", AIAA Journal, pp. 789-90, April, 1965.
- (12) Kaplan, W., Advanced Calculus, Addison-Wesley Publishing Company, Inc., Reading, Massachusetts, July, 1959.
- (13) Bulletin 37D, "Model HWB3 Hot-Wire Anemometer Theory and Instructions", Flow Corporation, Cambridge 42, Massachusetts, February, 1963.



- (14) Gassner, F. B., "A Method of Measuring Reynolds Stresses with a Constant Current Hot-Wire Anemometer", American Society of Mechanical Engineers Publication, United Engineering Center, New York, New York, 1965.
- (15) Eno, B. E., Sessions, O. T., and Kascoutas, T. F., "A Note on a Short Method of Measuring Reynolds Stresses with a Constant-Current, Hot-Wire Anemometer", Paper submitted to American Society of Mechanical Engineers, Journal of Applied Mechanics, 1966.
- (16) Brighton, J. A., "Artificially Thickened Turbulent Boundary Layers by Means of Wires", American Society of Mechanical Engineers Publication, United Engineering Center, New York, New York, 1965.
- (17) Parthasarathy, S. P. and Tritton, D. J., "Impossibility of Linearizing a Hot-Wire Anemometer for Measurements in Turbulent Flow", AIAA Journal, pp. 1210-11, May, 1963.
- (18) Tracy, H. J., "Turbulent Flow in a Three-Dimensional Channel," Proceedings of American Society of Civil Engineers, Journal of Hydraulics Division, pp. 9-37, November, 1965.

## APPENDIX A

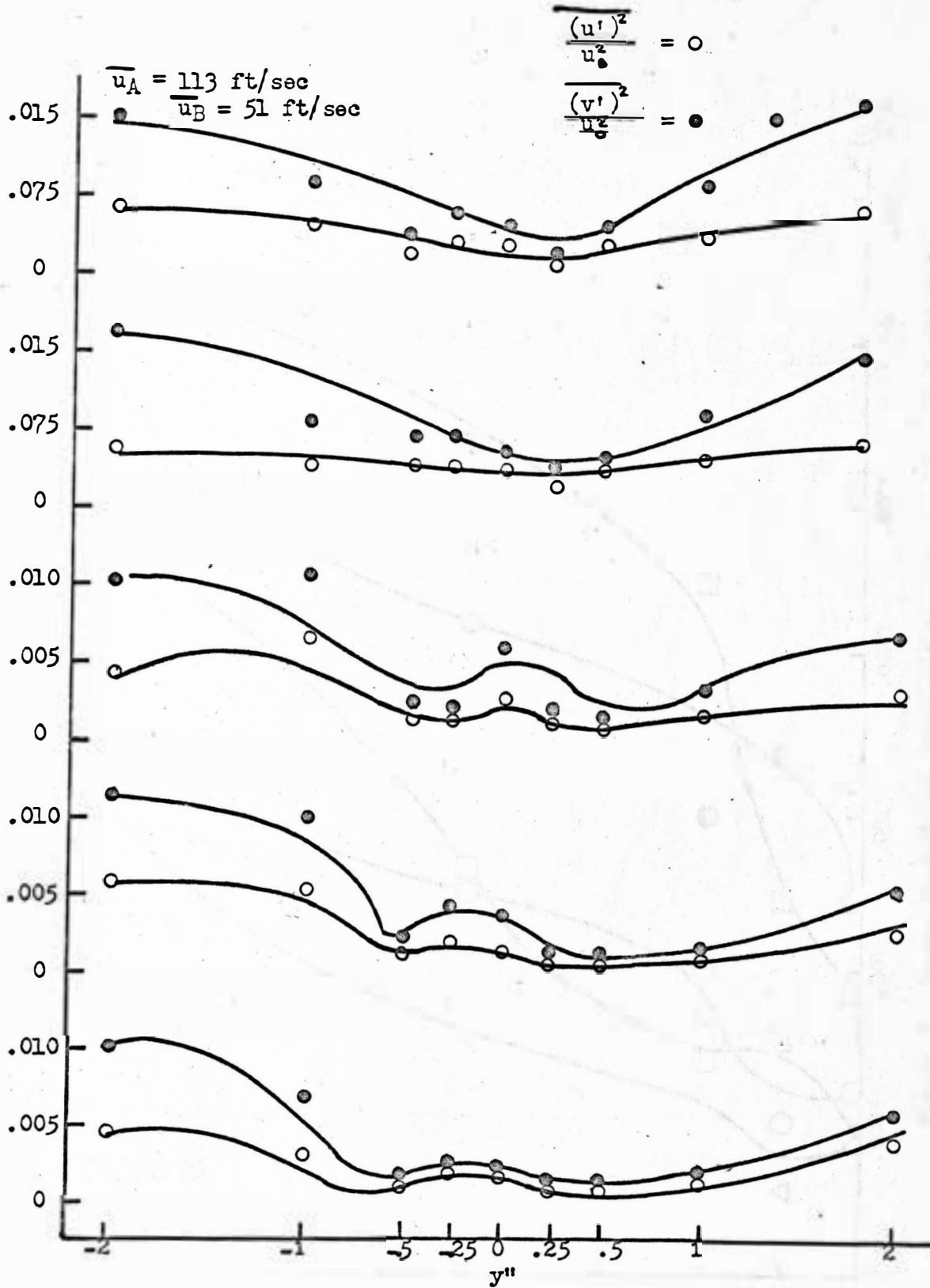


Figure 6. Comparison of Normal and Transverse Turbulence Components for  $\overline{u_A} = 113 \text{ ft/sec}$  and  $\overline{u_B} = 51 \text{ ft/sec}$

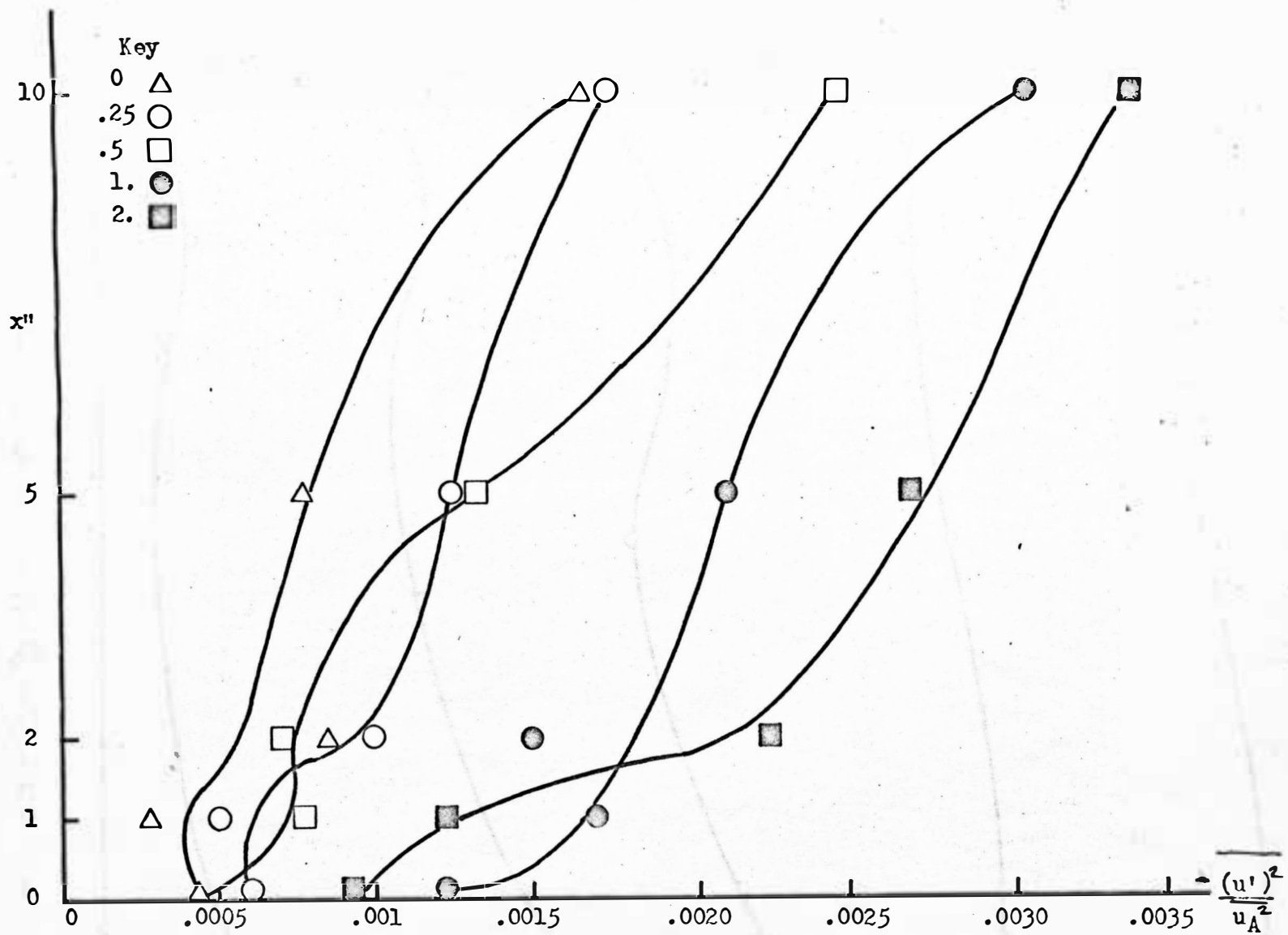


Figure 7. Normal Turbulence Component Profile for  $\bar{u}_A = \bar{u}_B = 110$  ft/sec

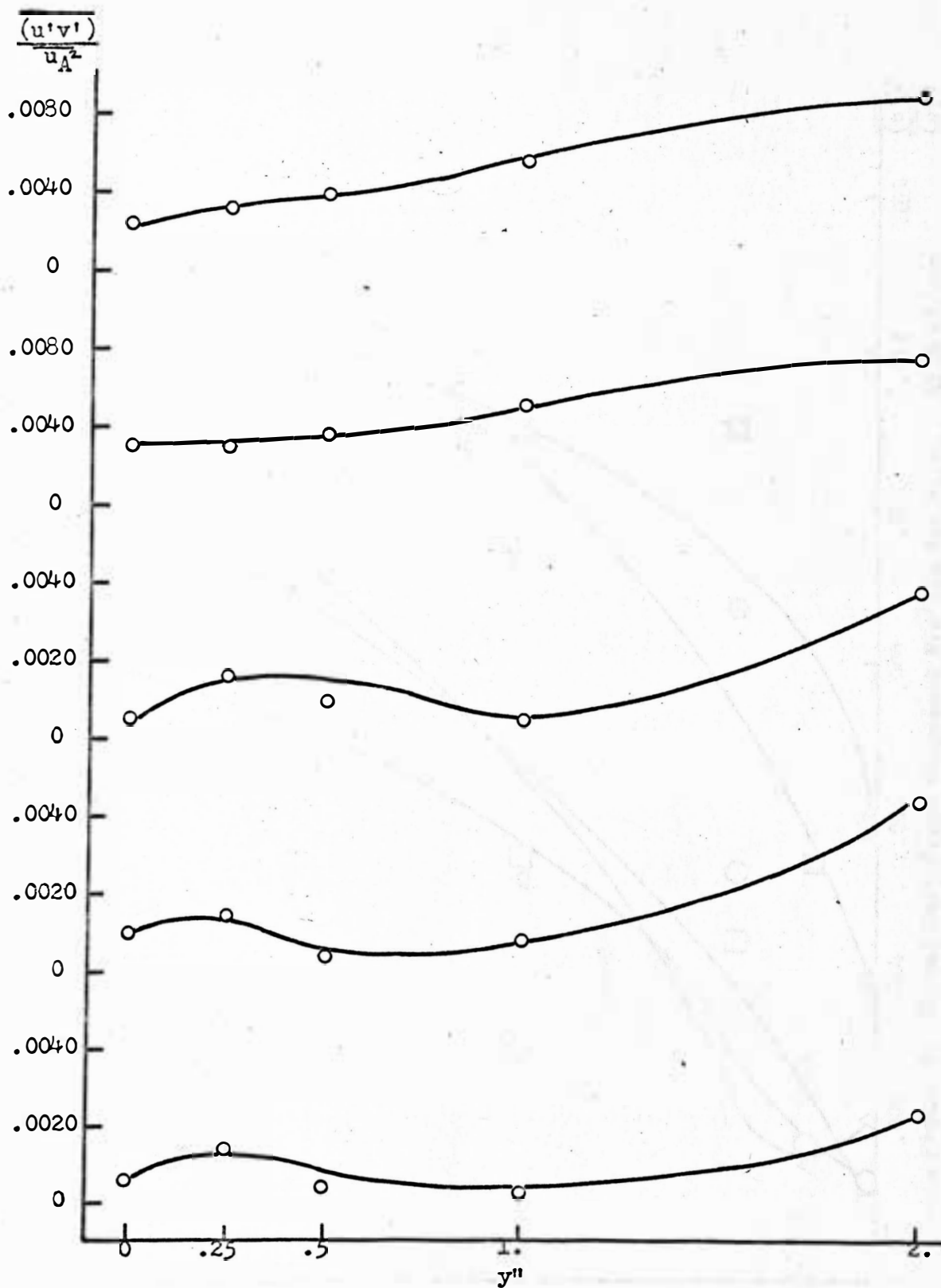
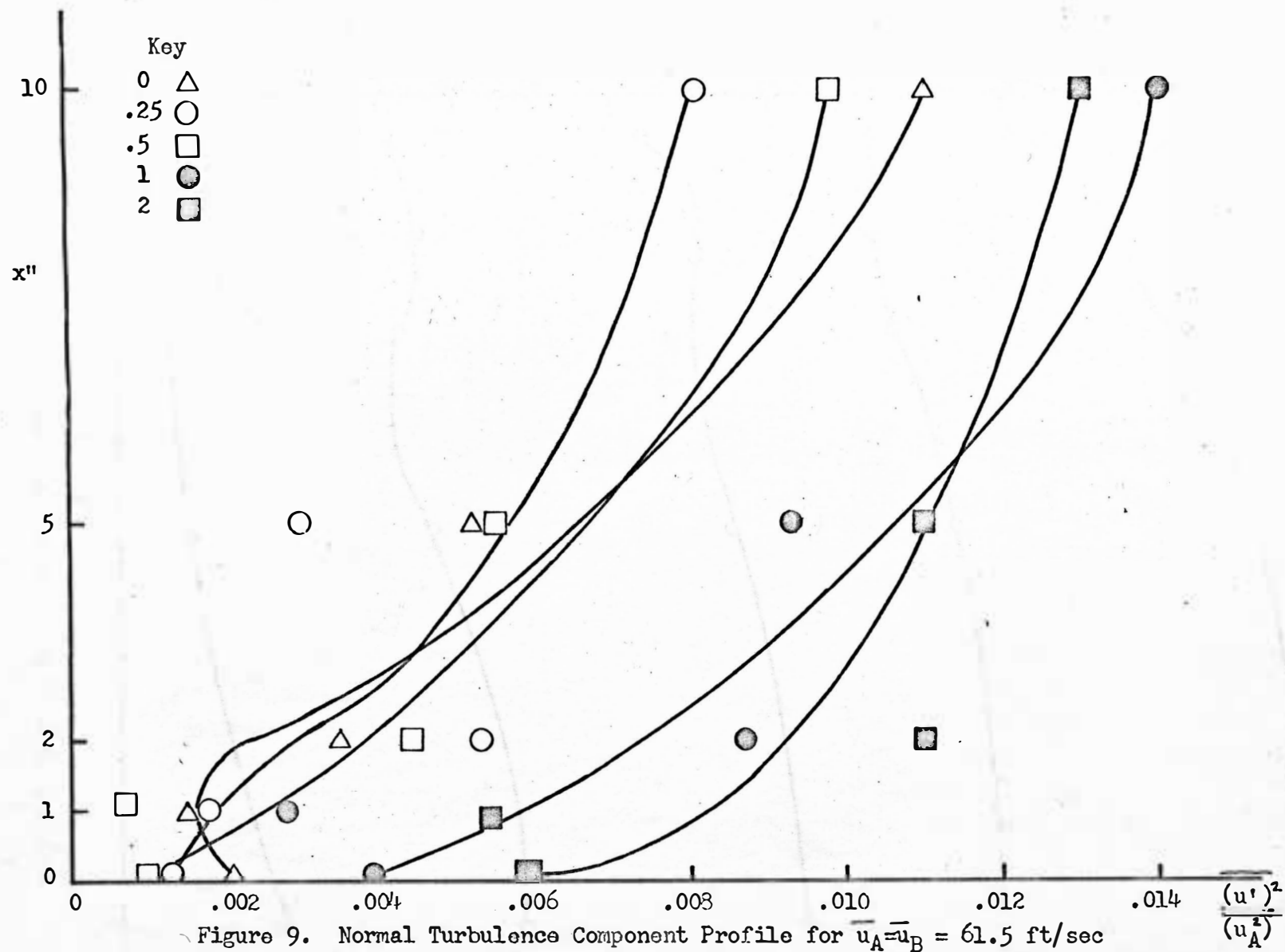


Figure 8. Apparent Shear Profile for  $\bar{u}_A = \bar{u}_B = 110$  ft/sec



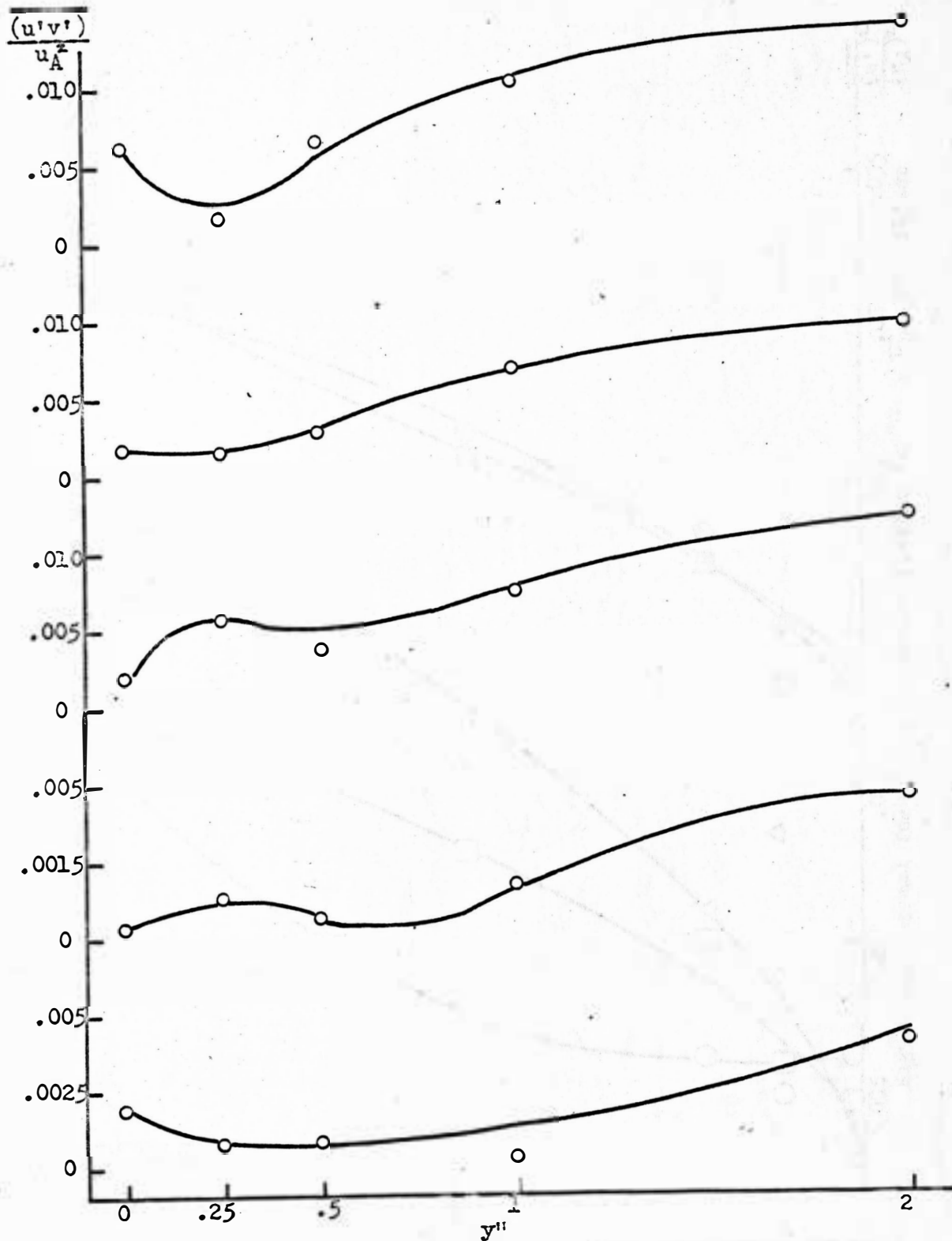
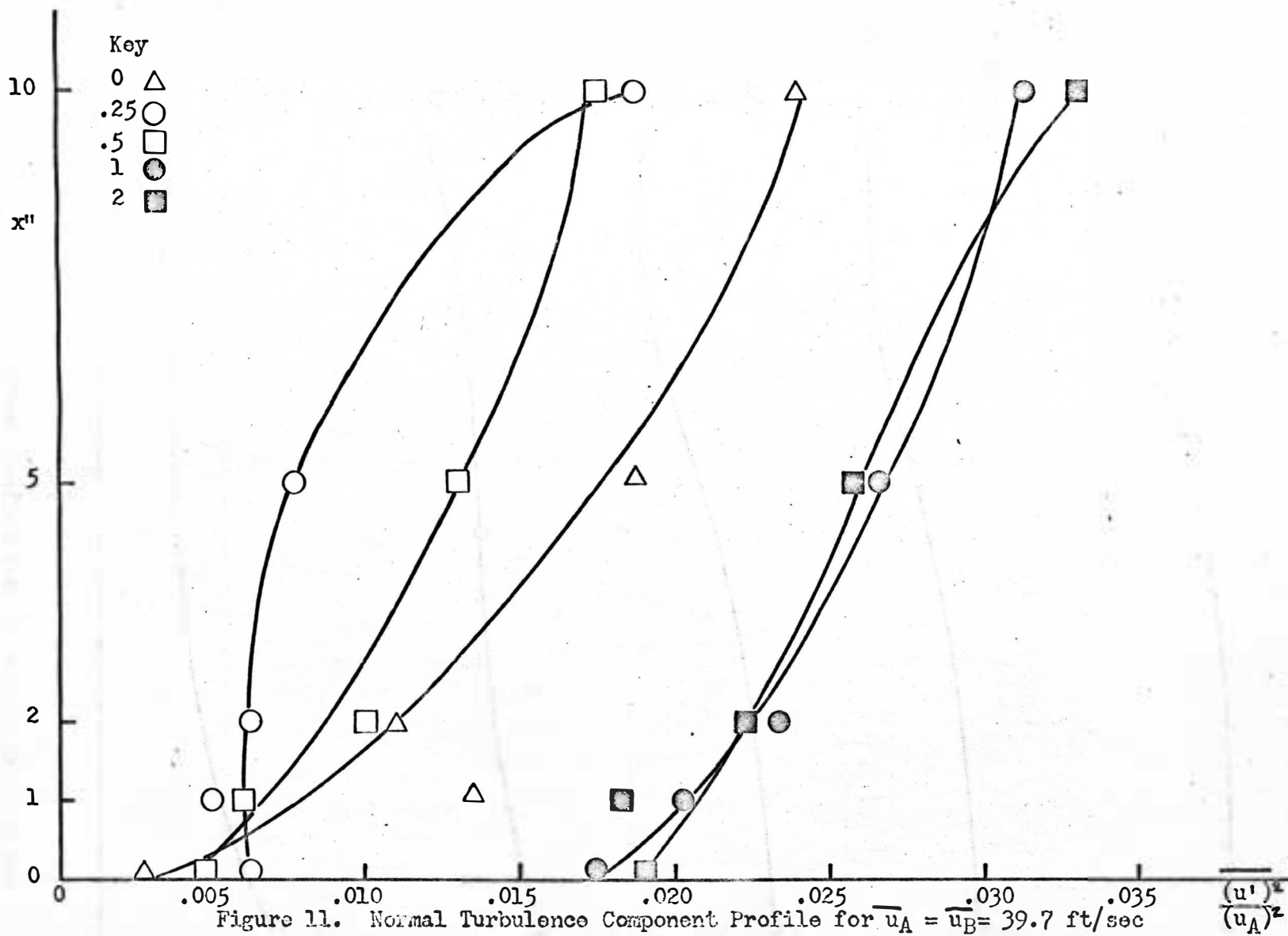


Figure 10. Apparent Shear Profile for  $\bar{u}_A = \bar{u}_B = 61.5 \text{ ft/sec}$





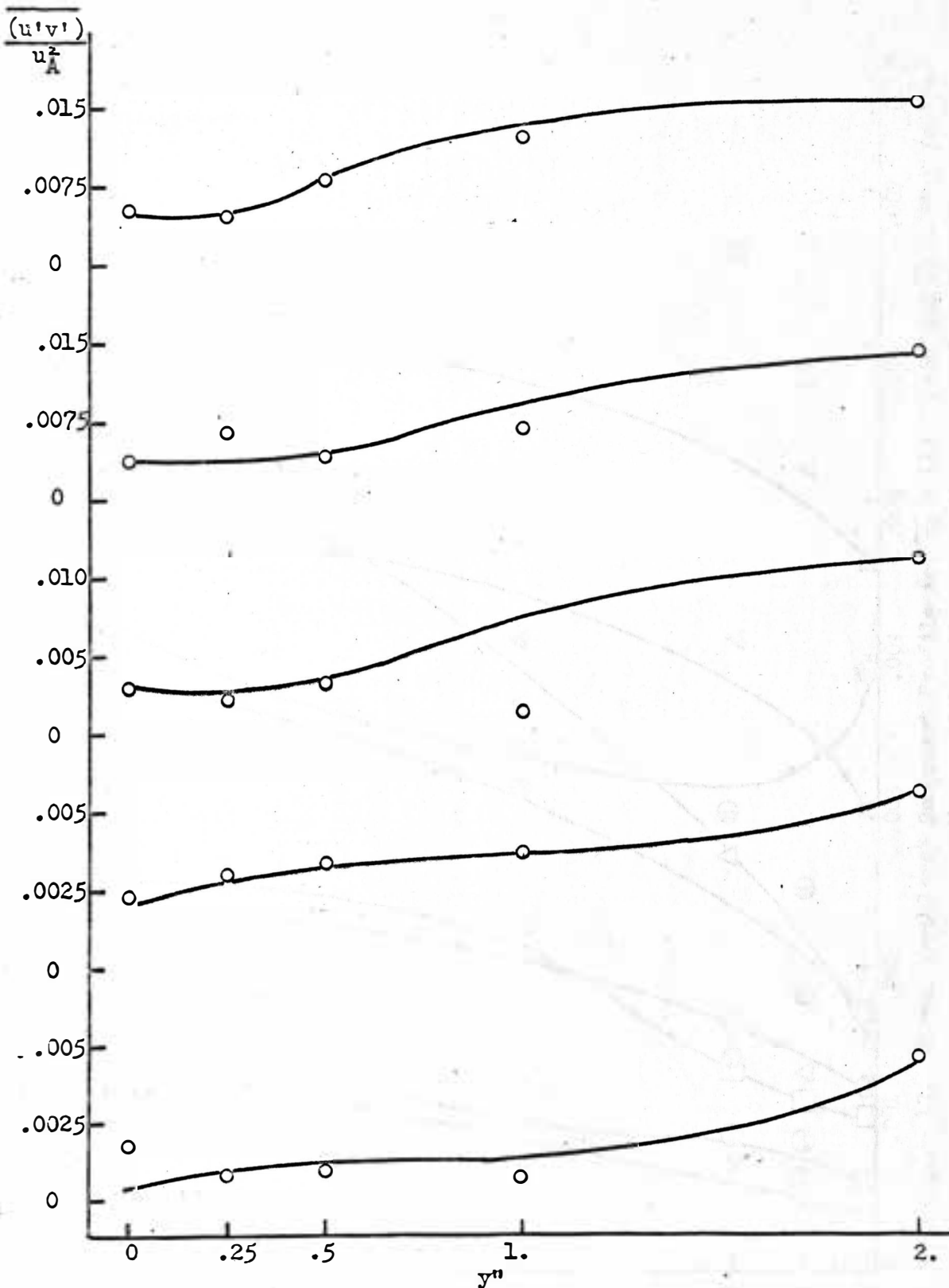
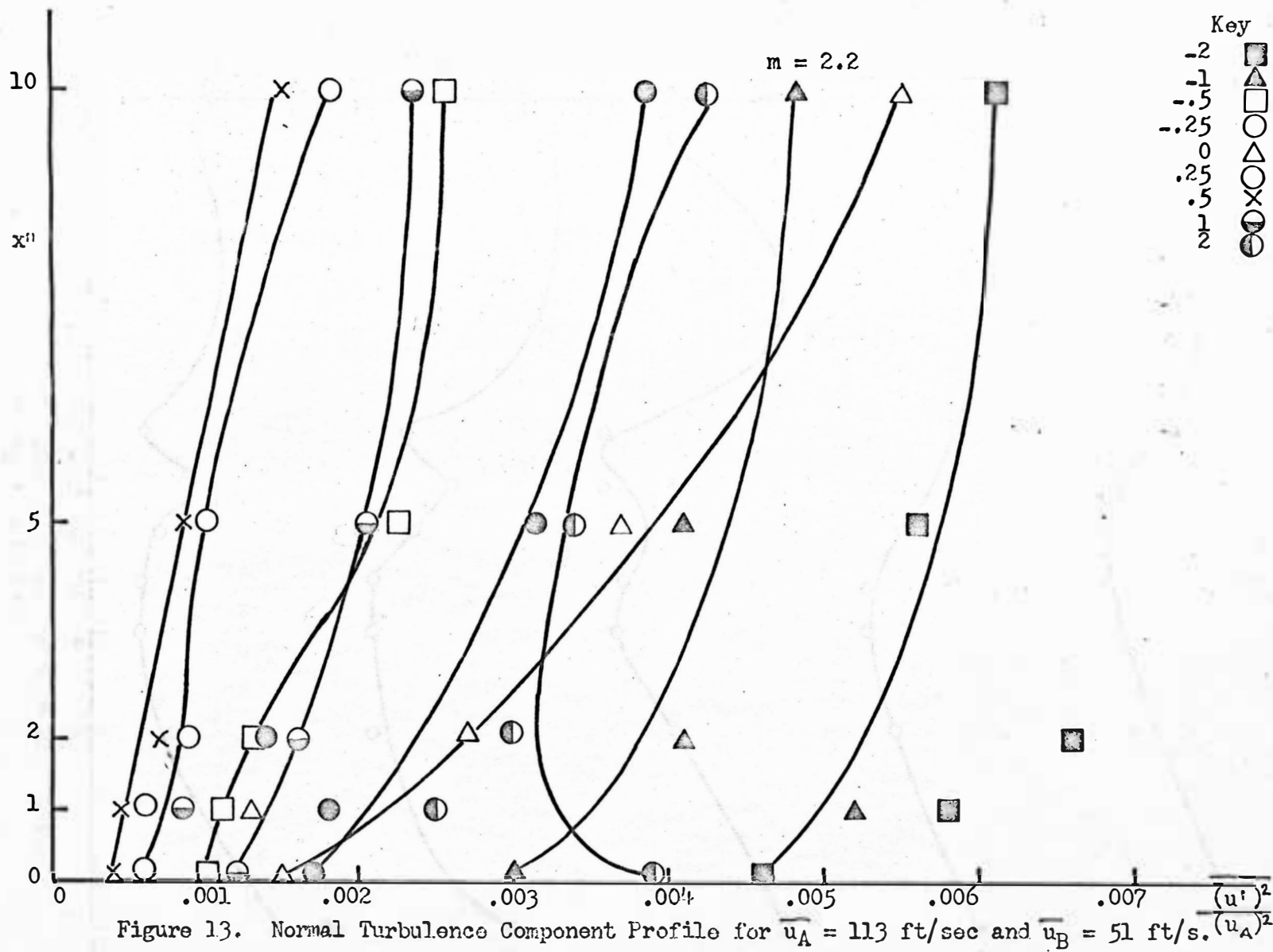


Figure 12. Apparent Shear Profile for  $\bar{u}_A = \bar{u}_B = 39.7$  ft/sec



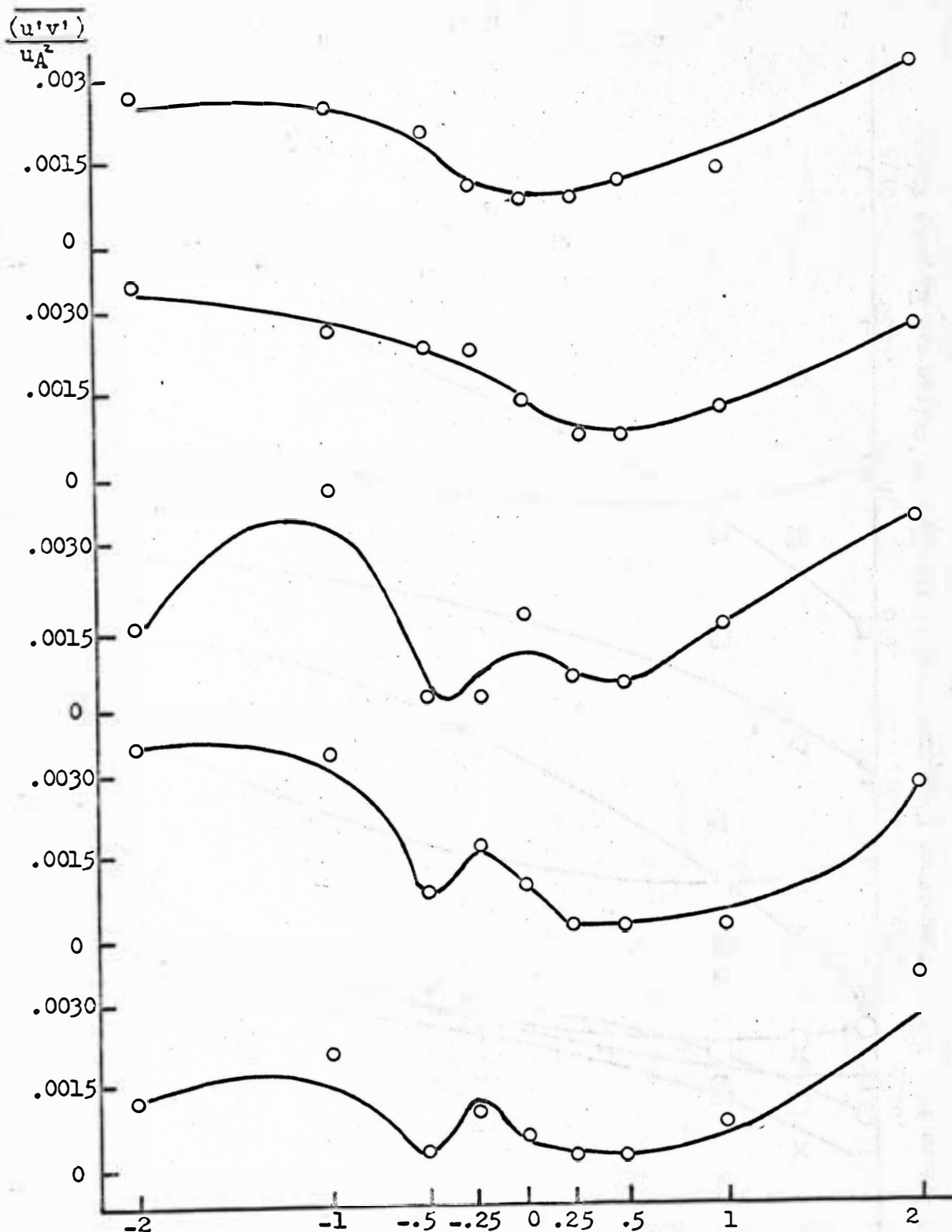
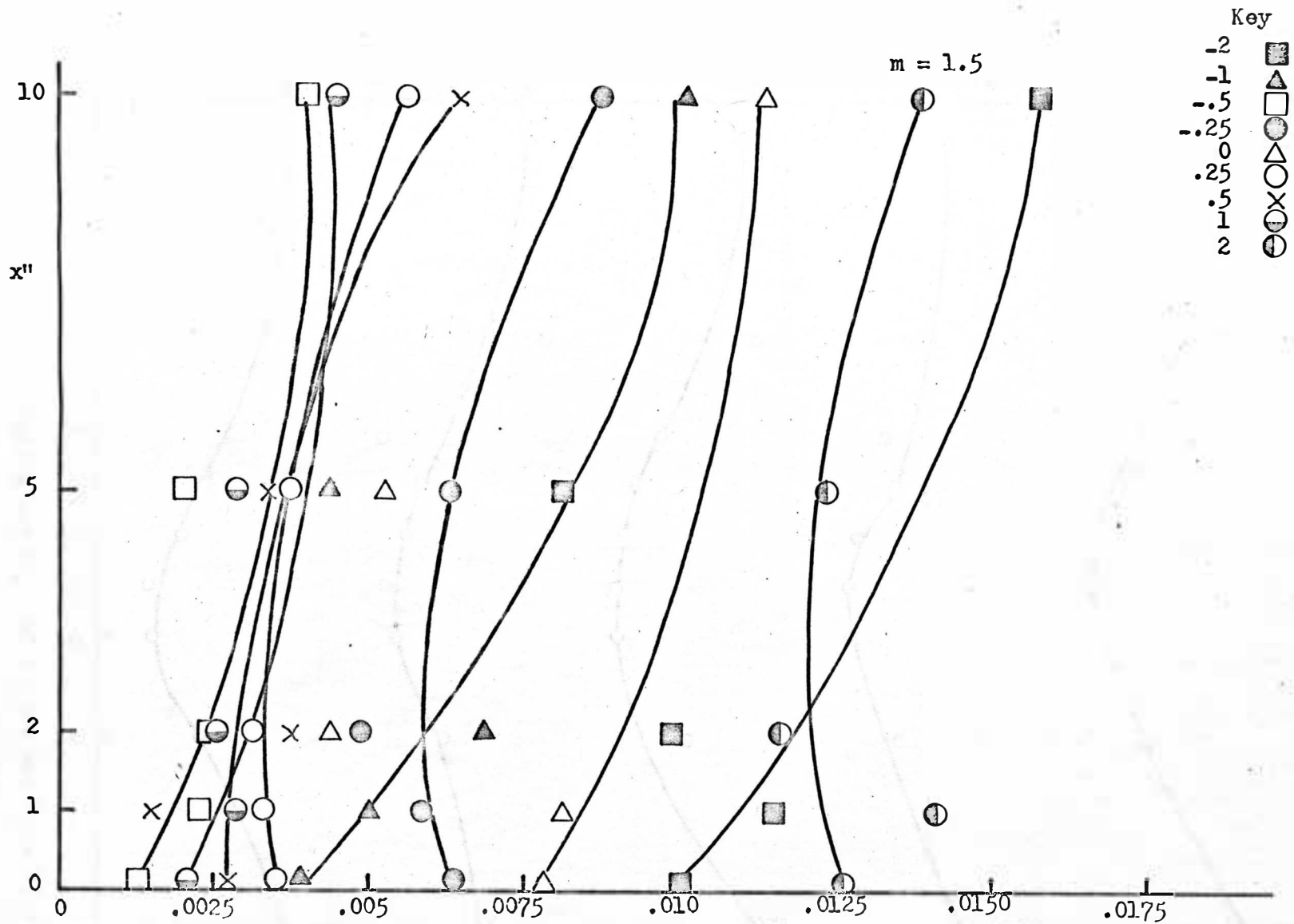


Figure 14. Apparent Shear Profile for  $u_A = 113$  ft/sec and  $u_B = 51$  ft/sec



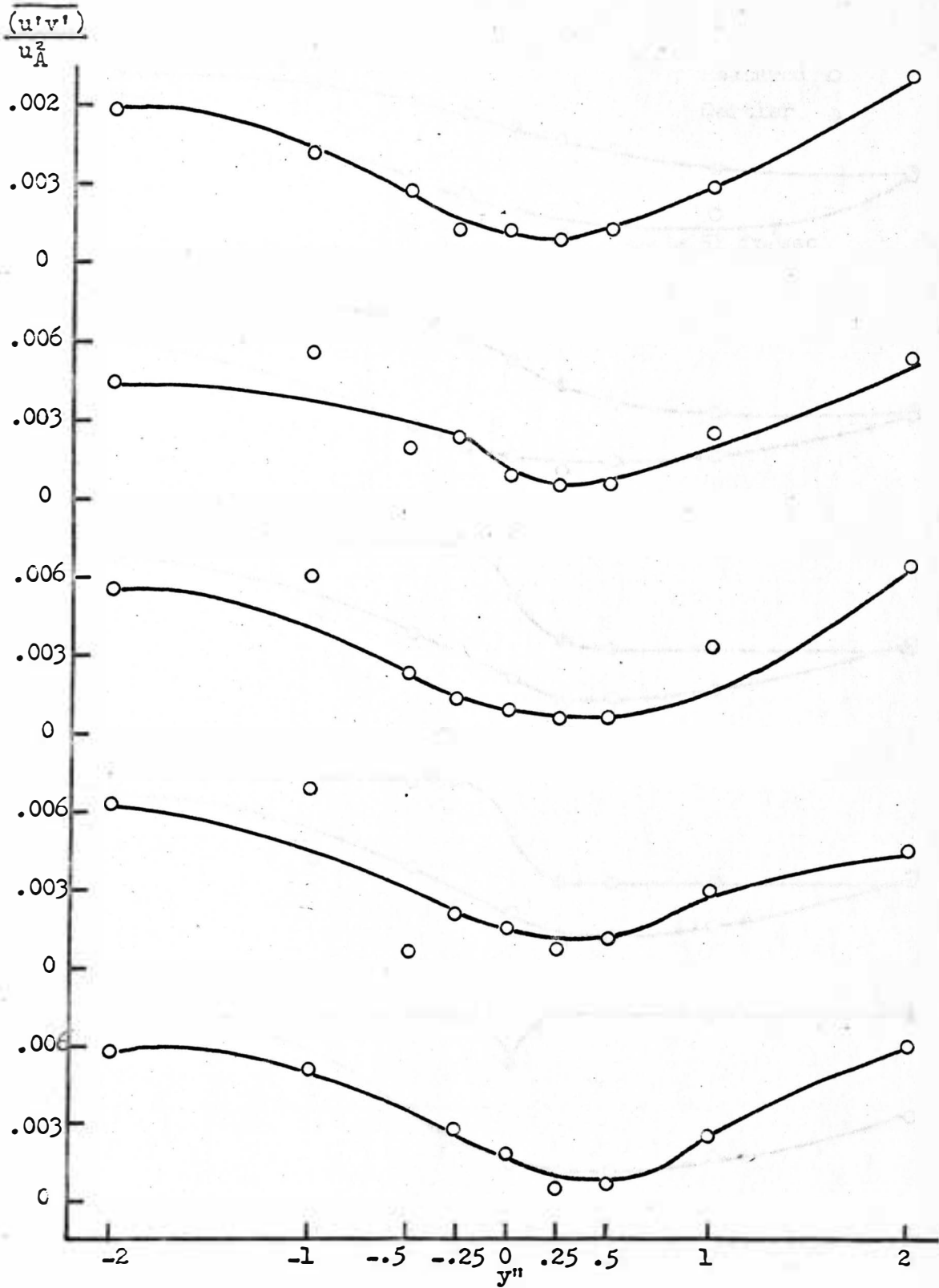


Figure 16. Apparent Shear Profile for  $\bar{u}_A = 67$  ft/sec and  $\bar{u}_B = 43$  ft/sec

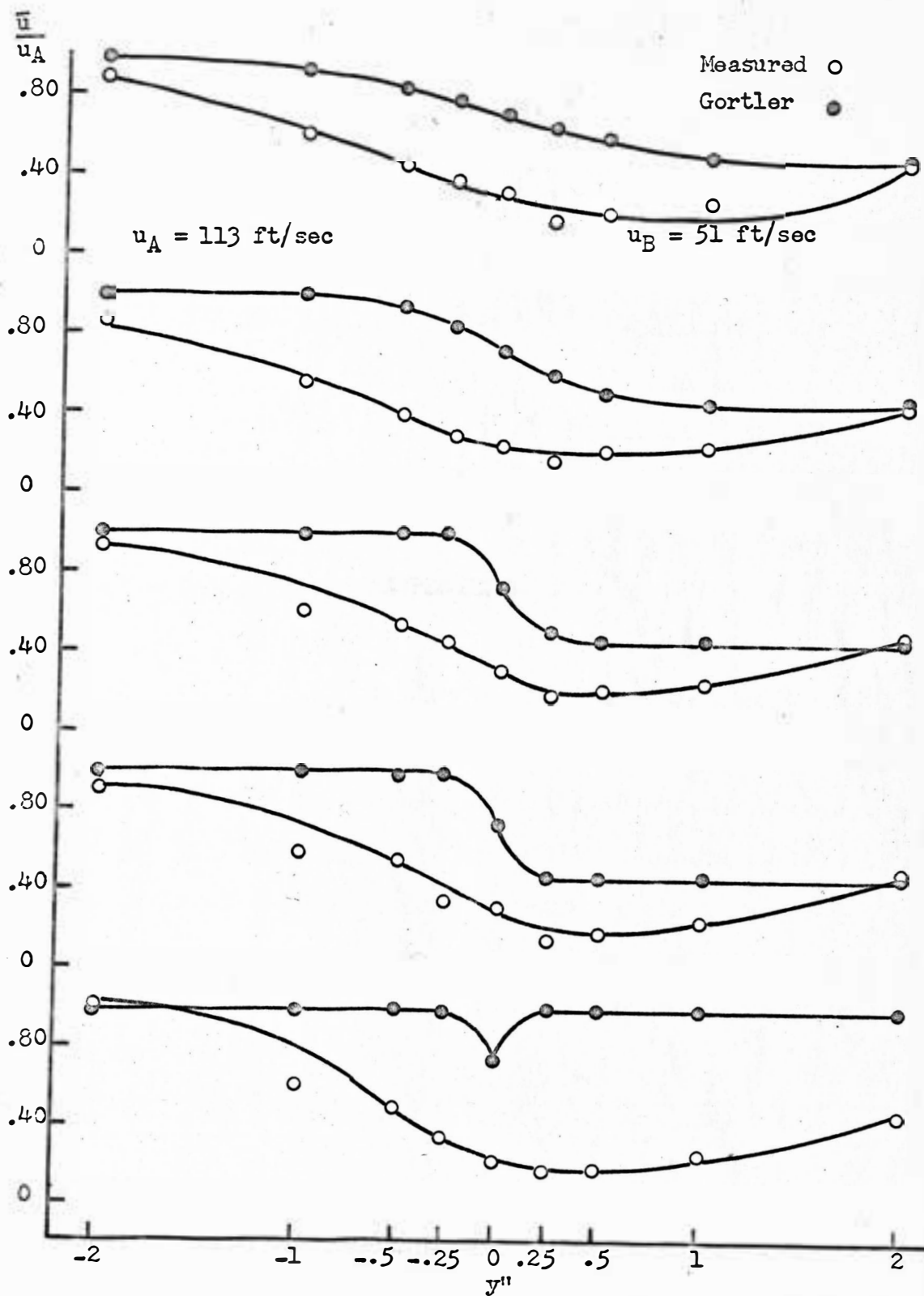


Figure 17. Comparison Between Measured and Gortler Velocity Profiles

## APPENDIX B

The collection and analysis of the information required to compute  $\frac{\overline{(u')^2}}{u_A^2}$ ,  $\frac{\overline{(v')^2}}{u_A^2}$ , and  $\frac{\overline{(u'v')}}{u_A^2}$  for each point is a lengthy process.

For example, nearly twenty-five minutes is required to gather the appropriate data for one point. Once collected, involved and repetitive relationships are necessary in the computation. Obviously, this is a situation which calls for (1) a shortening of the data gathering process and (2) computerization of the results.

A paper has been written by Gessner which deals with the first of these needs. He has developed a short method which reduces both the number of quantities to be measured and the ensuing equations. However, in his method, he makes several stringent assumptions. Those restrictions could not be fulfilled with any of the wires used in this study. Thus, an attempt was made to relax two of those restrictions so that this short method could be utilized.

The crux of the short method lies in the knowledge that  $\overline{(u')^2}$  can be evaluated by standard techniques (such as found in the Flow Corporation Bulletin). It will then be possible to determine  $\overline{(v')^2}$  and  $\overline{(u'v')}$  as functions of  $\overline{(u')^2}$  and the appropriate random signal voltmeter readings.

Consider the flow situation depicted in Figure 18. Assume that the level of turbulence is below 15%; then it is possible to write

$$\frac{c}{C} = \frac{u'}{U} + \frac{v'}{U \tan \beta} \quad (B-1)$$

and



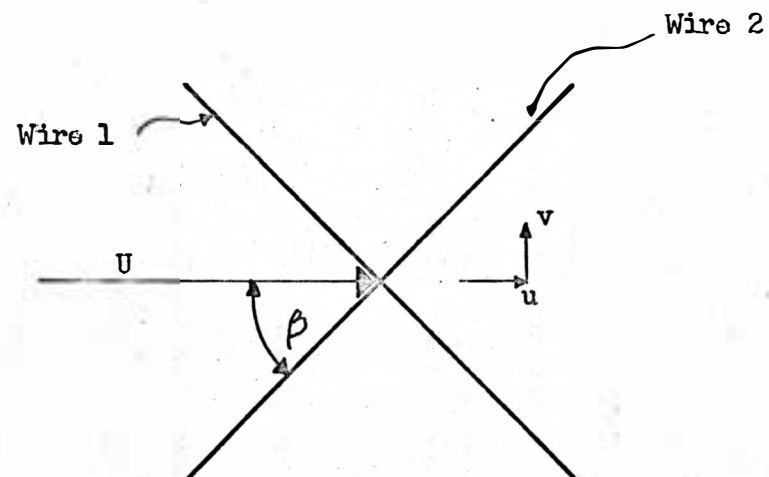


Figure 18. X-Wire Probe in a Typical Flow Situation

$$\frac{c_2}{C_2} = \frac{u'}{U} + \frac{v'}{U n_2 \tan \beta} \quad (B-2)$$

Gessner simplified (B-1) and (B-2) by assuming that  $n_1 = n_2 = 1$ .

However, the wires used in this study had values of  $(n)$  which approached 2.2 in many cases. Thus, in this analysis, the assumption will be that  $n_1 = n_2 = n$ . This seems reasonable because the cooling constant  $(n)$  is a function of the length to diameter ratio. The wires mounted on an X-array as shown in Figure 18 should have nearly identical geometries. Thus, the assumption seems reasonable.

Squaring equations (B-1) and (B-2) taking the mean time average and solving for  $\overline{(u')^2}$  and  $\overline{(v')^2}$  produces

$$\overline{(u')^2} = \frac{1}{4n^2(\sin\beta)^2/n} \left[ n^2 \overline{c_1^2} + 2n^2 \overline{c_1 c_2} + n^2 \overline{c_2^2} \right] \quad (B-3)$$

$$\overline{(v')^2} = \frac{n^2 \tan^2 \beta}{4n^2(\sin\beta)^2/n} \left[ \overline{c_1^2} - 2 \overline{c_1 c_2} + \overline{c_2^2} \right] \quad (B-4)$$

Cross multiplying (B-1) and (B-2) and taking a mean time average of the result produces a relationship for  $\overline{(u'v')}$ .

$$\overline{(u'v')} = \frac{\tan \beta}{4(\sin\beta)^2/n} \left[ n \overline{c_1^2} + n \overline{c_2^2} \right] \quad (B-5)$$

At this point, Gessner applied his second restriction. He set  $\beta = 45^\circ$ , thereby assuming the wire to be perpendicular. In the paper which was submitted, no restriction was made concerning the half angle  $\beta$ . Rather (B-3), (B-4) and (B-5) were left as functions of  $\beta$  and substituted into the following equations.

$$\overline{C_1^2} - \overline{C_2^2} = \frac{M_1^2 - M_2^2}{K_V^2 K_G^2 K^2} \quad (B-6)$$

$$\overline{C_1^2} + 2\overline{C_1 C_2} + \overline{C_2^2} = \frac{M_{1+2}^2 - M_n^2}{K_V^2 K_G^2 K_S^2 K^2} \quad (B-7)$$

$$\overline{C_1^2} - 2\overline{C_1 C_2} + \overline{C_2^2} = \frac{M_{1-2}^2 - M_n^2}{K_V^2 K_G^2 K_S^2 K^2} \quad (B-8)$$

Equations (B-6), (B-7) and (B-8) are written in accordance with Gessner's assumption that  $K_1 = K_2 = K$ . This means that the wires must exhibit near identity in their zero current resistances and in their velocity calibration curves. If this condition can not be met, then the only alternative is the previously mentioned technique presented in the Flow Corporation Bulletin.

Thus, proceeding with this assumption in mind and substituting (B-3), (B-4) and (B-5) into (B-6), (B-7) and (B-8), the following relations are produced

$$\overline{(v')^2} = \overline{(u')^2} \tan^2 \beta \left[ \frac{M_{1-2}^2 - M_n^2}{M_{1+2}^2 - M_n^2} \right] \quad (B-9)$$

$$\overline{(u'v')} = \overline{(u')^2} \eta \tan \beta \left[ \frac{(M_1^2 - M_2^2)(M_{1+2}^2 - M_{1-2}^2 - 2M_n^2)}{2(M_{1+2}^2 - M_n^2)(M_1^2 - M_2^2 - 2M_n^2)} \right] \quad (B-10)$$

Thus, a form is presented which allows calculation of  $\overline{(v')^2}$  and  $\overline{(u'v')}$  once  $\overline{(u')^2}$  is determined by standard techniques. The short method eliminates the switching of probes between the anemometer and sum-difference units. It also eliminates several readings in the data

collecting process. Finally the solutions (B-9) and (B-10) are considerably shorter than the Flow Corporation relations.

Equations (B-9) and (B-10) constitute an improvement over the Gessner solution in that the wire cooling constant and half angle are not predetermined. In line with Gessner, the assumption of well-matched wires is made. Unfortunately, none of the wires calibrated could be considered inherently well matched. Thus, no corroborative data can be presented at this time.